Development and Implementation of a 2-Dimensional Lake Model to Examine Arctic Lake Carbon Dynamics through the Holocene

Kassandra Reuss-Schmidt

June 2014

Development and Implementation of a 2-Dimensional Lake Model to Examine Arctic Lake Carbon Dynamics through the Holocene

by

Kassandra Reuss-Schmidt

Thesis submitted to the University of Southampton, UK, in partial fulfilment of the requirements for the degree of Master of Science in Geo-information Science and Earth Observation.

Specialisation: Environmental Modelling and Management

UNIVERSITY OF
Southampton

DECLARATION OF AUTHORSHIP

I, **Kassandra Reuss-Schmidt**, declare that the thesis entitled "**Development and Implementation of a 2-Dimensional Lake Model to Examine Arctic Lake Carbon Dynamics through the Holocene**" and the work presented in the thesis are both my own and have been generated by me as the result of my own scholarship. I confirm that:

- This work was done wholly while in candidature for a Masters degree at this University.
- Where any part of this thesis has previously been submitted for a degree or any other qualification at this University or any other institution, this has been clearly stated.
- Where I have consulted the published work of others accreditation has always been given.
- I have acknowledged all main sources of help.
- Where the thesis is based on work done by myself jointly with others, I have made clear exactly what was done by others and what I have contributed myself.
- It parts of this work have been published, they are listed below.

1. I have read and understood the University's Academic Integrity Statement for Students, including the information on practice to avoid given in appendix 1 of the Statement and that in this thesis I have worked within the expectations of this Statement.
http://www.calendar.soton.ac.uk/sectionIV/academic-integrity-statement.html

2. I am aware that failure to act in accordance with the Academic Integrity Statement for Students may lead to the imposition of penalties which, for the most serious cases, may include termination of programme.

3. I consent to the University copying and distributing my work and using third parties to verify whether my work contains plagiarised material. If a paper copy is also required for submission it must be identical to this electronic copy. Any discrepancies between these two copies may be considered as an act of cheating.

Signed ______________________ Date 28 May 2014

Disclaimer

This document describes work undertaken as part of a programme of study at the University of Southampton. All views and opinions expressed therein remain the sole responsibility of the author, and do not necessarily represent those of the University.

Abstract

The Arctic is currently undergoing widespread shifts in both the quality and distribution of vegetation, including the expansion of boreal forest and shrub-land at the expense of tundra. This trend, dubbed "Arctic Greening", is likely to significantly affect the amount of organic matter entering lakes and in turn carbon cycling in the Arctic. The extent of future shifts in climate and vegetation are presently unknown, however, a vast amount of paleo-proxy data and paleo-modelling enables one to reasonably approximate past conditions. To examine the effects of vegetation cover and climate change on arctic lake carbon cycling, output from the dynamic vegetation model LPJ-GUESS and the HadleyCM3 global circulation model have been linked to a 2-dimenstional lake model in order to simulate CO_2 efflux and sedimentation occurring back through the Holocene. This lake model, dubbed Paleo-Arctic Lake Model (PALM), had been developed for this thesis and is heavily derived from work done by Hanson *et al.* (2004) and Cardille *et al.* (2007).

To demonstrate that PALM provides realistic approximations of arctic lakes, the model was run over a range of *in situ* data for phosphorus, alkalinity, and incoming DOC and POC obtained from the Long Term Ecological Research (LTER) project. Modelled efflux and sedimentation fell within a reasonable range. A sensitivity analysis was also performed which revealed that the efflux was most sensitive to changes in the volume and concentration of DOC entering the lake, lake temperature, and the respiration rate of producers. Sedimentation was most affected by the average particle diameter, the amount of aerial carbon input, and the respiration rate of producers.

Once the model was validated it was applied to two lakes, Lake AT1 in Greenland, and Ruppert Lake in Alaska. The lakes were simulated during time periods where paleo-data indicated that their catchments were dominated by differing vegetation types, specifically 2,000, 6,000, 7,000, 9,000, 11,000, and 14,000 years before present. PALM simulated significantly different ($P<0.05$) sedimentation and efflux in a number of this time slices. Finally, the sedimentation output from Ruppert Lake was compared to a lake core extracted from the site. While the carbon sedimentation rate was underestimated by an order of magnitude, the coupled modelling approach does appear to reproduce the pattern of sedimentation change observed in Ruppert Lake.

Acknowledgements

I would like to thank the European Commission for financing this study through the Erasmus Mundus Scholarship and my supervisors, Mary Edwards and Jadu Dash, for patiently consulting me throughout this endeavour.

My thanks also goes out to all those who have provided data for this project, namely: the BRIDGE research group at the university of Bristol, specifically Dan Lunt, for making their paleo climatic datasets available for use, the University of Alaska in Fairbanks, specifically Nancy Bigelow for her help regarding the bathymetric data, and Mitch Slife and Dayne Broderson for making the SPOT 5 image of Ruppert available, the members of the LAC project especially Kim Davis and Maarten Van Hardenbroek for providing data, information, and advice.

Furthermore, I give my thanks to Alex and Grigoris for their support and advice in editing this document.

Finally, I would like to thank my family, for inspiring my curiosity about the world and always supporting me as I try to figure it out.

Table of Contents

List of figures

List of tables

Introduction

1.1 Lakes and the Global Carbon Cycle

Lakes and other inland freshwaters are recognized as major components of the global carbon cycle (Cole *et al.*, 2007, Tranvik *et al.*, 2009, Romankevich and Vetrov, 2013). It is estimated that 1.9 Pg of carbon enter lake systems annually (Cole *et al.*, 2007). This carbon is then either exported via rivers and streams, enters lake sediment, or is emitted as the greenhouse gases carbon dioxide (CO_2) and methane (CH_4). The amount of CO_2 efflux from terrestrial freshwaters is similar in magnitude to oceanic CO_2 uptake (Tranvik *et al.*, 2009), with the CO_2 resultant from manmade reservoirs alone accounting for 4% of anthropogenic CO_2 emissions (St Louis *et al.*, 2000). While carbon efflux from lakes increase the earth's potential for global warming, lake sediments act as a primary long term carbon sink. The amount of organic carbon entering lake sediments outpaces the rate of burial in the ocean by a factor of three (Tranvik *et al.*, 2009). Though lakes cover around 3% of the continental land surface (Downing *et al.*, 2006), it is estimated that their sediments contain 820 Pg of carbon (Cole *et al.*, 2007). The balance in lakes between carbon sedimentation and efflux is influenced by many factors such as pH, ion/nutrient composition, temperature, and the concentration of organic matter (Sommer *et al.*, 2012). In the wake of climate change and anthropogenic landscape transformation, lakes will likely experience significant changes in their catchments possibly resulting in shifts in their carbon balance (Lurling and Domis, 2013, Cardille *et al.*, 2009, Domis *et al.*, 2013). As scientists set forth to predict environmental change it is imperative to have a more complete understanding of the global carbon cycle, the role lakes play therein, and how that role may change in the future.

1.2 Arctic Lakes and Climate Change

Understanding lake carbon cycling is of critical importance in the Arctic not only because it is a lake rich region, but also because the Arctic is disproportionately affected by global warming, showing increases of mean annual temperature occurring at twice the rate of the global average (Achberger *et al.*, 2011). About one fourth of earth's lakes are located in the Arctic (Jones, 2013). Lakes comprise on average 5% of total regional surface cover (Paltan Lopez, 2013), with certain regions, such as the coastal area north of the Brooks range in Alaska, showing upwards of 50% lake cover (Kling *et al.*, 1992). These lakes are highly significant to regional carbon cycling. Average CO_2 evasion from lakes in Finland, estimated at 1.4 Tg C, was equivalent to 20% of the average C accumulation rate in Finnish forest in both biomass and soils (Kortelainen *et al.*, 2006). Algesten *et al.* (2004) observed 21 Scandinavian catchments and found that in-lake mineralization accounted for 30% to 80% of terrestrial carbon loss.

Factors influencing lake carbon cycling, such as temperature, precipitation, fire frequency and the amount of catchment carbon are predicted to significantly change in the Arctic during the upcoming decades (Thorsteinsson and Pundsack, 2010, McGuire *et al.*, 2009). Increases in temperature should generally boost carbon sequestration as it will enable higher rates of primary production within lakes via longer grow periods (Domis *et al.*, 2013). However, increases in precipitation and catchment carbon concentrations will likely increase carbon loading into lakes (Thorsteinsson and Pundsack, 2010, Benoy *et al.*, 2007). This influx of catchment carbon would lead to higher rate of carbon efflux (Cardille *et al.*, 2009) and a complex set of interactions with the planktonic primary producers within the lake (Brett *et al.*, 2012, Hessen *et al.*, 2004, Roiha *et al.*, 2012).

Vegetation cover has expressly been implicated to affect lake organic carbon concentrations (Sobek *et al.*, 2007, Klimaszyk and Rzymski, 2013). Significant shifts in vegetation cover, and thus catchment carbon content, are already being observed in the Arctic. For example, McManus *et al.* (2012) showed an average increase in Leaf Area Index (LAI) with a value of 0.2 between 1986 and 2010, with shrub-tundra LAI increasing from 20-80%. In a review of 22 papers Epstein *et al.* (2013) summarises the main trends observed, namely, increased evidence for greening based on Normalized Differential Vegetation Index (NDVI), changes in plant community composition, changing phenology, an increase in tall shrubs in low artic ecosystems, and browning occurring mostly in arctic boreal forest. The observed changes in vegetation cover and quality are likely included in local and landscape scale feedback loops, involving surface energy, carbon fluxes, water balance, and plant-herbivore interactions. Furthermore, terrestrial vegetation models indicate that these trends are likely to continue (Epstein *et al.*, 2013). Results from modelling exercises show an NDVI increase and the northward advancement of shrub and boreal forest boundary into tundra dominate areas (Zhang *et al.*, 2013b, Miller and Smith, 2012, Pearson *et al.*, 2013).

1.3 Current Project

1.3.1 Lakes and the Arctic Carbon Cycle (LAC)

One approach to deriving the key regulators of the lake carbon cycle and lake systems in general is the analysis of information stored in lake sediments. This branch of study is called paleolimnology. Lake cores contain an abundance of information, to name but a few, past plant cover can be deduced from macro fossils and pollen data (Brubaker *et al.*, 2009, Higuera *et al.*, 2009), plant cover can in turn be used to approximate ancient climate conditions (Garreta *et al.*, 2012), charcoal fragments can be used to reconstruct fire regimes (Higuera *et al.*, 2011), chironomids can be used to construct a record of past lake eutrophication (Luoto and Ojala, 2014), sediments may even reveal past dissolved organic matter concentrations (Rouillard *et al.*, 2011). With the wealth of available information from sediment cores, a paleolimnological study focused on Arctic lakes, with a known history of vegetation cover change, would seem to be a good place to start understanding how current vegetation cover change might affect Arctic carbon cycling in the future. That in fact is the goal of the Lakes and the Arctic Carbon Cycle (LAC) project. The LAC projected has currently cored lakes in a variety of locations spread across the Arctic. LAC members are analysing these cores in order to determine:

1. The role past catchment vegetation cover, as defined by plant functional types (PFTs), played in the concentration of organic matter in lakes.

2. The extent to which past carbon dynamics are a function of the biotic components of lakes.

3. If changes in catchment composition cause are key drivers of lake’s ecological state and carbon dynamics.

The LAC project will examine lake cores containing records going back to slightly before the beginning of the Holocene epoch, which corresponds to shortly after de-glaciation from the last glacial maximum.

1.3.2 Scope

This modelling exercise fits into the broader LAC project by allowing comparison between observed paleo-data and simulated results, for which all assumption are known. I have set forth to create a modelling system that integrates land-cover and climate change into a lake carbon cycling model.

Aim: To simulate carbon sedimentation and CO_2 efflux through the Holocene and validate modelled results through comparison to the actual sediment record.

Research Objectives:

1. Identify time periods in the modelled lake's history during which distinct vegetation types were dominate.

2. Develop a lake carbon cycling model applicable in the Arctic, referred to hence forth as the Paleo Arctic Lake Model (PALM).

3. Model catchment carbon via a terrestrial vegetation model (Arctic version of LPJ-GUESS).

4. Approximate paleoenvironmental conditions for the catchment to use as input data for LPJ-GUESS and PALM.

5. Link PALM to LPJ-GUESS to simulate land cover effects on carbon sedimentation and efflux.

Research Questions:

1. Does PALM simulate reasonable carbon fluxes?

2. Can LPJ-GUESS model modern and paleo-vegetation in a realistic manner?

3. Is the output from LPJ-GUESS a suitable input for PALM?

4. Does vegetation cover change and do shifts in climate affect lake carbon cycling?

5. Can the coupled lake carbon cycling models simulate historic carbon sedimentation?

1.4 The Lacustrine Carbon Cycle

Lake carbon cycling is comprised of a myriad of acid-base and redox chemical reactions which in turn are affected by multiple factors such as organic carbon runoff, plankton, aquatic plants, the benthic community, nitrogen and phosphorus fertilization, calcium carbonate and other mineral runoff, precipitation mediated carbon deposition, lake morphology, fish, turbidity, heterotrophic and anaerobic bacteria, lake temperature, and piston velocity. The goal of any modelling exercise is to reduce a system's complexity. This is done by capturing the driving forces behind a process, while not including details which don't significantly increase the model's predictive power. With a system as complex as the lacustrine carbon cycle it is important to single out its most important components.

1.4.1 Aqueous Carbon Chemistry and Stratification

In oxygenated water, where aerobic conditions exist, the cycling of dissolved inorganic carbon (DIC) is regulated by the acid base reactions of the CO_2-Bicarbonate-Carbonate system (Figure 1). Of these three compounds only aqueous CO_2 is in equilibrium with the atmosphere, while the other compounds remain in solution. Depending on the pH and acid neutralising capacity (ANC), the equilibrium between these compounds will shift allowing differing levels of DIC to stay within solution (Baird and Cann, 2005). Aerobic conditions do not, however, always exist within lakes. During the warmer months of the year a lake will often become stratified or split into distinct thermal layers. This is due to the fact that water has its maximum density at 4° C. The only way for stratification to be avoided is for perturbing forces, such as mixing caused by wind, to physically mix the warmer less dense water with the colder denser water trapped below. Through this mechanism the mixing layer, or epilimnion, is continuously exposed to atmospheric oxygen and thus remains oxygenated. However, the bottom layer, hypolimnion, slowly becomes depleted of oxygen leading to anaerobic conditions under which CH_4 is produced. The horizontal plane separating the two lake layers during stratification is called the thermocline. Thermocline depth has been shown to play a significant role in lake carbon cycling (Weyhenmeyer *et al.*, 2012, Fortino *et al.*, 2014). One of the main reasons why the balance between aerobic and anaerobic conditions affects lake carbon cycling is its control over the aerobic respiration of CO_2 and anaerobic respiration of CH_4 by the biotic component of the lake. To constrain its scope, this project elected to focus on aerobically produced efflux. Therefore, CH_4 production is not explicitly considered.

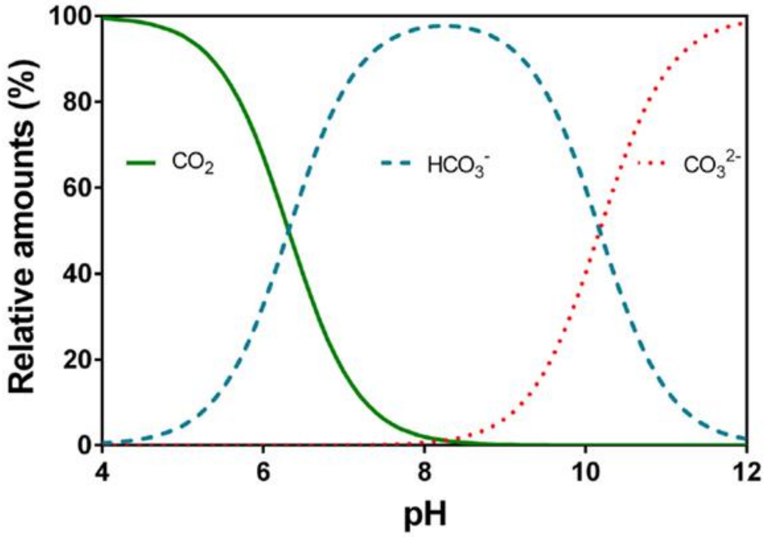

Figure 1. Inorganic carbon exists in various dissolved forms, the ratio of which is control in part by the pH of the water in question. To know the amount of CO_2 being emitted from body of water information about pH or a related index like alkalinity must be known. Figure reproduced from Baird and Cann (2005).

1.4.2 Biotic Component, Phosphorus, and Trophic State

Gross primary production (GPP) is the net conversion of light energy into chemical energy, typically in the form of fixed carbon, by a biotic community. The amount of GPP occurring within a lake is integral to its carbon fluxes because it uses the DIC pool within the lake as a carbon source. If gross primary productivity is high enough the depletion of the DIC pool may be so great that CO_2 no longer effluxes into the atmosphere but rather draws down into the lake (Pacheco *et al.*, 2013). This lake state only occurs when the nutrient availability within a lake is high enough. The productivity within a lake is limited by a number of factors but the most important one is nutrient availability. In fact, a lakes' biotic state can be classified by the concentration of nutrients they have. High productivity lakes are titled eutrophic, medium as mesotrophic, and low productivity lakes as oligotrophic. Though aquatic systems can be limited by nitrogen (Kortelainen *et al.*, 2013), phosphorus is almost without exception the limiting nutrient within lakes (Grimm *et al.*, 2003). Furthermore, 80 % of DIC consumed by primary producers, i.e. autotrophs, is metabolized and respired back into the DIC during the course of a day (Hanson *et al.*, 2004). The lakes biotic component also contains an abundance of heterotrophic organisms. Heterotrophic organisms gain their energy by breaking down and respiring the carbon fixed by producers as well as other organic material that enters the lake system.

1.4.3 Organic Carbon

Dissolved and particulate organic carbon are key factors controlling freshwater chemistry and ecology. They, in many cases, determine whether the lake's planktonic community is primarily heterotrophic or autotrophic (Hessen *et al.*, 2004, Cardille *et al.*, 2007, Lottig *et al.*, 2011). Due to its absorptive nature, the pigmentation in dissolved organic carbon (DOC) hinders photosynthesis through the entrapment of photons (Steinberg *et al.*, 2006, Hessen *et al.*, 2004). Particulate carbon also reduces light penetration within the water column (Hanson *et al.*, 2011). Organic carbon (OC) also acts as a substrate for heterotrophs. Heterotrophs break down OC, mineralizing it into DIC, a significant fraction of which is CO_2 that is then degassed back into the atmosphere (Hanson *et al.*, 2011, Hanson *et al.*, 2004, Algesten *et al.*, 2004). Studies have derived an approximate threshold value for DOC, 5 mg L^{-1}, after which lakes tend toward heterotrophy (Jansson *et al.*, 2000, Prairie *et al.*, 2002). DOC also affects the mixing layer or thermocline depth of lakes (Fee *et al.*, 1996, Hanson *et al.*, 2004, Cardille *et al.*, 2007). As DOC absorbs light it increases water temperature in close proximity, thus stimulating circulation and increasing mixing layer depth. Though an oversimplification of the interactions between OC and the planktonic community, this illustrates the mechanisms by which OC concentration affects a lake's carbon balance, shifting it from being productive and autotrophic to a heterotrophic CO_2 source.

1.5 Modelling Lake Carbon Cycling

1.5.1 Existing Models

Many different types of models seek to simulate at least some components of the lake carbon cycle. These models range from complex dynamic ecosystem models, such as PCLake which incorporates a myriad of components that can be seen in Figure 2 (Mooij *et al.*, 2010), and hyper focused models like PEG that deal with the dynamics between plankton species (Sommer *et al.*, 2012).

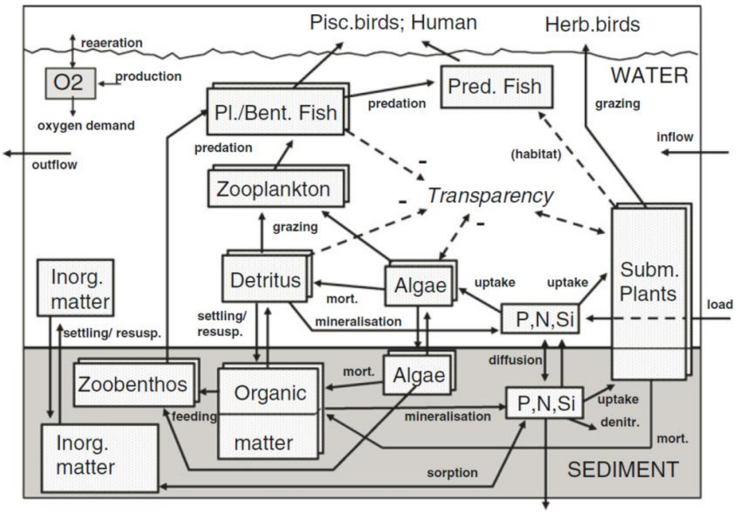

Figure 2. Representation of the lake ecosystems model PClake. Figure taken from (Mooij *et al.*, 2010).

Other lake models, which may not model carbon dynamics, simulate aspects of the lake, like temperature, that greatly influence carbon cycling. For example, Perroud and Goyette (2012) assessed four one dimensional lake temperature models to assess their ability to accurately model thermocline depth and the respective temperatures of the epilimnion and hypolimnion. Another example would be the work done by Deng *et al.* (2013) that models how the physics of wind perturbation influences carbon efflux. However, of the multitude of existing lake models few incorporate both the modelling of lake ecosystems and the modelling of DOC, POC, DIC, carbon efflux and sedimentation. Even with all the complexity modelled in PClake it does not expressly model DIC or its flux to the atmosphere (Mooij *et al.*, 2010). Some models that do incorporate these components are the coupled CE-QUAL-W2 (Cole and Buchak, 1995), CAEDYM-DYRESM model (Gal *et al.*, 2009), Delft3D-ECO (Los, 2009), and LUWI (Cardille *et al.*, 2007). The Delft3D model contains representations of DOC, POC, DIC and CO_2 efflux and was developed to model the effect of sediment transport and lake morphology on carbon cycling. It has since been adapted into the Delft3D-ECO model to include biotic components and the carbon stocks (Los, 2009). CE-QUAL-W2, a 2-water quality model, models nitrogen (N), various forms of OC, phosphorus (P), dissolved gases such as oxygen and CO_2, chlorophyll-a content, and with an optional biotic add-on can model plankton dynamics as well as aquatic vegetation (Cole and Buchak, 1995, Mooij *et al.*, 2010). The Computation Aquatic Ecosystem Dynamic Model (CAEDYM) coupled with the Dynamic REServoir simulation model (DYRESM) is capable of modelling POC, sediment fluxes, lake nutrients including N, P, and silicon, 8 different plankton types, fish, benthic communities and it has been widely used for modelling long term carbon dynamics including sedimentation and efflux (Gal *et al.*, 2009, Makler-Pick *et al.*, 2011, Parparov and Gal, 2012). All of these models have been applied to model water quality in numerous studies to great effect. However, this is generally done in areas where much is already known about the water bodies in question and the models can be calibrated to the specific system. As input data is limited, due to the remote nature of our study sites as well as the time span over which the model should be applied, a less complex lake carbon cycling model was chosen which had been applied to lakes with limited accessible input data. The Lake Uplands/Wetlands Integrator (LUWI) model was developed to model the hydrological and carbon dynamic of over 7000 lakes in a lake rich region in northern Michigan (Cardille *et al.*, 2007). It is much more generalized than the previously mentioned models and estimates the GPP of the lakes biotic component based mostly on total phosphorous concentration. LUWI is also capable of modelling carbon sedimentation and efflux, but it does not distinguish between incoming DOC and POC. However, previous work done on the same lake area included POC and DOC cycling and could be used to adjust LUWI (Hanson *et al.*, 2004).

1.5.2 Application of Aquatic Models in the Arctic

No lake models, applied specifically in the Arctic, modelled lake POC and DOC concentrations, the efflux of CO_2, and sediment formation were discovered in the literature. However, models were found that modelled aspects of the freshwater carbon cycle. For example, Dillon and Molot (1997) successfully applied a simple mass-balance model to simulate DOC concentrations in lakes in Ontario Canada. Futter *et al.* (2007) developed the Integrated Catchments Model for Carbon (INCA-C) family of models which simulate carbon fluxes from catchments into streams. While the literature review was not exhaustive and a suitable lake carbon model tailored to the Arctic may exist, the lack of a model explicitly built for modelling carbon dynamics in the Arctic led to our adaptation of the temperate lake carbon models (Cardille *et al.*, 2007, Hanson *et al.*, 2004) for application in the Arctic.

1.6 Modelling Catchment Carbon

As this exercise aims to model the effects of vegetation cover change on catchment carbon the focus of research has been on vegetation models that simulate catchment carbon stocks. There are other widely used approaches to modelling catchment carbon stocks that disregard the expressed modelling of vegetation (Shao *et al.*, 2013) but they fall beyond the scope of this project.

1.6.1 A Review of Arctic Vegetation Modelling

There have been a number of modelling approaches used to simulate vegetation cover and terrestrial carbon cycling in the Arctic. A review by Kittel *et al.* (2000) summarizes three of the major types of models utilized to simulate the Arctic's response to possible climate forcing. Equilibrium Biogeographic Models function by modelling the vegetation distribution at equilibrium with a given set of climatic conditions. Examples of these models include BIOME3 (Haxeltine and Prentice, 1996), MAPSS (Neilson, 1995), and DOLY (Melillo *et al.*, 1995). These models focus heavily on modelling physiological responses, given a set of rules and processes, with the aim of maximizing a parameter, such as: leaf area index, MAPSS, net primary productivity, or BIOME3. Equilibrium models are accurate at modelling plant responses and have been widely used, however, they are unsuitable for this study as they do not simulate time dependent responses. Frame-based transient ecosystem models focus on the likelihood of a given cell to transition between one vegetation type to another. Starfield and Chapin (1996) applied the transient model ALFRESCO to simulate vegetation shifts in the Arctic due to warming. This type of model proved highly effective at modelling vegetation transitions, but it does not model plant interactions within a grid-cell and does not incorporate detailed biogeochemical cycling. Another type of model, that merges the equilibrium and transient models, is the Dynamic Global Vegetation Model (DGVM). DGVMs are able to model time-step dependent transition and include detailed biogeochemical processes. Some DGVMs that have been applied to the Arctic include HYBRID (White *et al.*, 2000), IBIS (Foley *et al.*, 1996), LPJ (Sitch *et al.*, 2003), and MC1 (Daly *et al.*, 2000). While there was some observed variation between the results they shared a number of general trends. All of the DGVMs showed a marked decrease in tundra under arctic warming scenarios, due to the expansion of shrub-land and the pole-ward migration of boreal forest. Of the models reviewed, subsequent iteration of the LPJ model were tailored to function on a local scale and adapted with a focus on modelling the Arctic (see LPJ-GUESS, Benjamin Smith 2001). Modification to the LPJ model included the addition of permafrost dynamics (Wania *et al.*, 2009) and arctic specific vegetation types (Miller and Smith, 2012). The specification and a more thorough description of this model can be found in section 3.4 of the methods.

1.6.2 The Versatility and Validation of LPJ-GUESS

LPJ-GUESS is widely used, modified, and evaluated in a multitude of studies addressing various topic from the impacts of climate change (Zhang *et al.*, 2013b), the effects of fire on vegetation (Pfeiffer *et al.*, 2013), to whether or not the vegetation post last glacial maximum could support mega-fauna in Europe (Allen *et al.*, 2010). Projects utilizing LPJ-GUESS that are relevant to this study, either because of their validation of the model or due to their addition of a potentially useful module, are seen in Table 1.

Table 1. A subset of studies is shown which are relevant to this project's use of LPJ-GUESS, either for developing novel functionality or validating the model.

Author	*Importance*
(Sitch *et al.*, 2003)	Evaluated LPJs performance on a global scale.
(Miller *et al.*, 2008)	Modelled sites in the Scandanavian Arctic back through the Holocene.
(Wania *et al.*, 2009)	Incorporated permafrost and improved soil hydrology.
(Ahlstrom *et al.*, 2012)	Investigated how LPJ-GEUSS responded to climate inputs from forcing from almost 20 different climate models.
(Huntley *et al.*, 2013)	Explored the interation of LPJ-GUESS with the global circulation model HadCM3 through the last glacial maximum.
(Zhang *et al.*, 2013b, Pearson *et al.*, 2013)	Modelling results predicting future PFT shifts in the Arctic.
(Tang *et al.*, 2013)	Incorporated topography into the model to improve modelled hydrology.

1.7 Coupling Catchment and Lake Carbon Dynamics

Carbon found in lakes is either a product of the biotic element of the aquatic system, called autochthonous carbon, or is transported to the lake from terrestrial sources, called allochthonous carbon. The quantification of allochthonous carbon loading into lakes has long been a source of error in lake carbon cycling models (Cardille *et al.*, 2007). Therefore, much effort has been put into quantifying DOC and POC export from catchments into lakes.

1.7.1 Quantification of Catchment-Lake Interactions

Linking the terrestrial carbon pool to freshwater carbon cycling, to a large degree, has only been done fairly recently (McDowell, 2003). This is primarily due to knowledge gaps concerning decomposition and the factors effecting carbon transport. Various attempts were made to quantify the fluxes of carbon and link them to specific factors. Previously the amount of DOC and POC entering a given lake was thought to depend on the catchment's geography, the upland and wetland flow paths, soil type, and vegetative land cover (Neff and Asner, 2001, Hanson *et al.*, 2004, McDowell, 2003). Sobek *et al.* (2007) analysed 7,514 lakes spread over 6 continents to derive a multiple linear regression explaining 40% of observed DOC variability. Sobek's regression incorporates mean annual runoff, altitude, and soil carbon density. Buffam *et al.* (2011), based on the work of previous researchers in the NHLD, created a complete carbon budget showing the flow of carbon between the atmospheric, terrestrial, and aquatic portions of their study area. Their results confirmed the importance of lakes as carbon storage, as lakes, along with peat-containing wetlands, housed more than 80% of the total carbon pool while only covering 13% and 20% of their study area respectively. The paper asserted that approximately 5% of total NEE entered into the NHLD's lakes where about 1/3 of the carbon became sediment while the rest effluxed into the atmosphere. There have also been many studies focused on specific cover types and their DOC production. Aitkenhead-Peterson *et al.* (2003) examined over 70 different studies spanning the globe from the tropics to the polar region which examined DOC production in different cover types. The deposition of POC has also been quantified in studies in a variety of regions, from the Great Lakes in the US to remote Arctic Lakes in

Siberia (Eisenreich *et al.*, 1981, Dickens *et al.*, 2011, Teodoru *et al.*, 2013).

1.7.2 Integrating Catchment Carbon in Modelled Lake Systems

In 2009 Mckay *et al.* cited the need for a fully integrated atmosphere-catchment-lake model for the purpose of constraining the contribution of lakes to global warming. Cardille *et al.* (2007) was among the first studies to couple the carbon stocks of a terrestrial vegetation model to a lake model. However, this model does not expressly simulate soil DOC production and its export to aquatic systems. Very recently such models, capable of modelling DOC production and sorption, have been developed. For example, Zhang *et al.* (2013a) developed an extension to the forest hydrology model ForHyM2 that was able to model the concentration of DOC in a coniferous and deciduous site in Canada. Wu *et al.* (2013) developed the TRIPLEX-DOC, which proved highly effective in temperate pine forests, and is calibrated to function with 11 other species/genera of trees. The model developed by Wu *et al.* (2013) went one step further and coupled the DOC export model to a 2-dimenstional lake model, developed based off the CO_2 efflux model crated by Cole *et al.* (2010). Wu's coupled lake model would be ideal for this work; however, it only models forest cover, neglecting other vegetation types such as shrubs or herb tundra, and it does not model sedimentation since it is focused on DOC and CO_2 dynamics. Recent work has also coupled the CE-QUAL-W2 model with the hydrology model SWAT (Debele *et al.*, 2008). The Soil Water Assessment Tool (SWAT) is a hydrological model that models the export of nutrients, pollutants, metals and carbon from on the drainage basin scale of lakes, rivers and streams. This model was developed by the US Department of Agriculture for modelling the impacts of agriculture on surrounding water systems and has been fully linked to ArcGIS (http://swat.tamu.edu/). SWAT outputs have proven to be compatible with CE-QUAL-W2 and capable of modelling lake volume with a high degree of success, $R^2>0.8$, with slightly less success in modelling other variables like oxygen and chlorophyll concentration. SWAT, like CE-QUAL-W2, is a model that requires a relatively large amount of input data to run. Furthermore, Debele *et al.* (2008) did not evaluate the coupled models capability to model sedimentation, carbon efflux, or even DIC concentration. LPJ-GUESS models some decay processes, such as fine root formation and decomposition and the heterotrophic respiration of differing litter pools with their own decay rates (Wania *et al.*, 2010). Similar methods of modelling soil decomposition were used by Zhang *et al.* (2013a) and by Wu *et al.* (2013). As LPJ-GUESS can model Arctic PFTs it was deemed a good candidate for coupling to a lake carbon model.

Materials and Methods

2.1 Study Sites

Lake coring sites for the LAC project were selected to show pan-Arctic variability. These sites exhibit a range of current vegetation cover that span from boreal forest, a biome rich very carbon, to steppe tundra whose catchments have extremely low carbon stocks. Based on data availability two of the LAC sites, namely Ruppert Lake in Alaska and Lake AT1 in Greenland, were chosen for this modelling exercise (Figure 3).

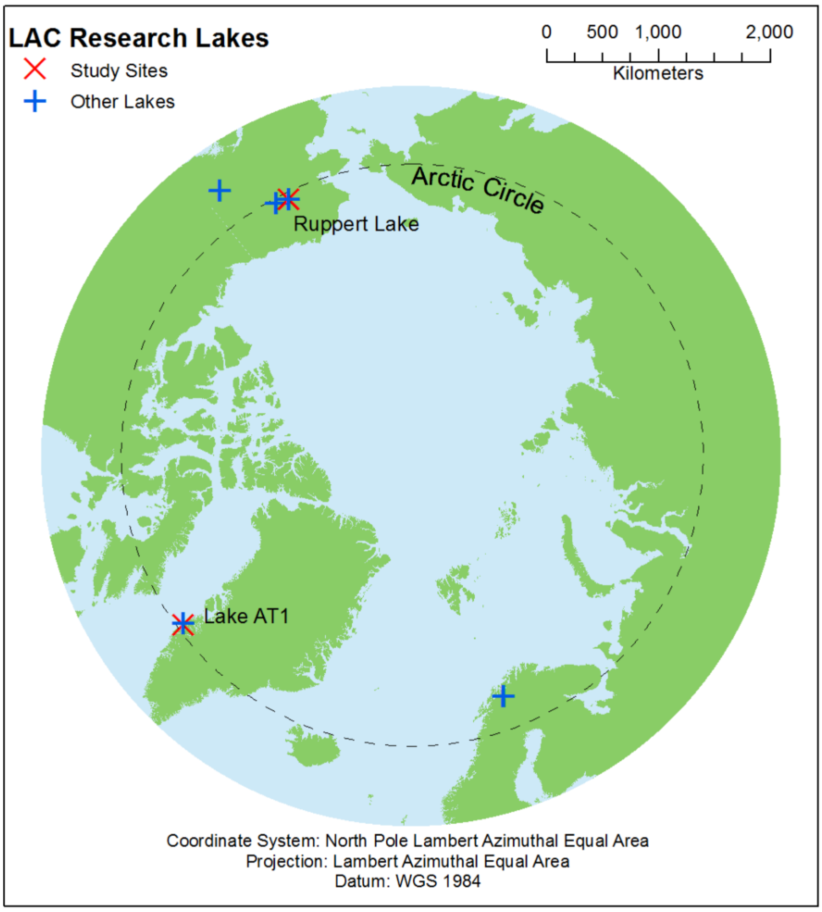

Figure 3. LAC research lakes, shown as blue crosses, are distributed throughout the Arctic. This study focuses on two of the lakes, shown via the red x symbols, Lake Ruppert in Alaska and Lake AT1 on the southwest coast of Greenland.

2.1.1 Ruppert Lake

Ruppert Lake is a relatively shallow small, nutrient poor lake located at the Southern base of the Brooks Mountain Range in central Alaska (Figure 4, Table 2). This inland site has average summer temperatures of about 15° C and winter temperatures around -25° C, though minimum recorded temperatures can drop to nearly -40° C. The lake is a postglacial non-thermokarst lake situated in an array of glacial moraines. Lake formation likely occurred between 16,000 and 17,000 calibrated years before present (cal yrBP)[1]. The lake is fed by a small stream in the north of the catchment which is surrounded by upland forests and shrub-land. An outflow stream in southwest end drains Ruppert into the larger adjacent Walker Lake. Forests in the catchment are comprised of *Picea glauca, Betula papyrifera* and *Populus tremuloides* which share the uplands with shrub-lands consisting of *Alnus* spp., *Salix* spp., and *Betula glandulosa*. The upper portions of the moraines are vegetated with *Vaccinium* spp., *Dryas* sp., lichen spp., and moss cover. Low lying permanent wetlands surround the lake and exist along the inflow and outflow streams. These areas are dominated by *Carex* spp. and *Sphagnum* spp. (Edwards, 2013).

2.1.2 Lake AT1

Lake AT1 is, like Ruppert, also a small shallow nutrient poor lake, though it is larger and does have a higher phosphorus concentration in comparison to Ruppert (Figure 4, Table 2). The DOC concentration at the site, is however, significantly lower than at Ruppert. The lower DOC concentration is likely due to the fact that AT1's catchment is sparsely vegetated with large areas of exposed bedrock (Liversidge, 2012). Vegetation cover is dominated by prostrate dwarf shrubs, namely *Salix gluauca* and *herbacea*, with a smattering of heathland exhibiting *Empetrum* spp. and Ericaceae. Lake AT1 is in a coastal area and exhibits much milder climate conditions than Ruppert. The average temperature range at the site is between -12° and 7° C (Anderson *et al.*, 2012). Lake formation occurred between 11,000 and 10,000 cal yrBP (Anderson *et al.*, 2012).

---

[1] It should be noted that calibrated years BP refers to calibrated carbon-14 (^{14}C) radio carbon years, where 1950 is designated as present at it is the advent of radio carbon dating. Calibrated years BP, yrBP, should more or less correspond to their calendar counterpart given the addition of 1,950 to account for the shift between the year 1950 BCE and 0 BCE.

Table 2. Location as well as relevant lake and catchment properties for Ruppert Lake and Lake AT1.

Lake	Latitude	Longitude	Catchment area (ha)	Lake area (ha)	Mean Depth (m)	TP (ug/L)	DOC (mg/L)	ANC (meq/L)
Ruppert	67.071461	-154.244039	39.34	3.74	2.1	3.46	8.39	1.25
AT1	66.967517	-53.401583	150	11	8.25	13.9	1.27	0.5

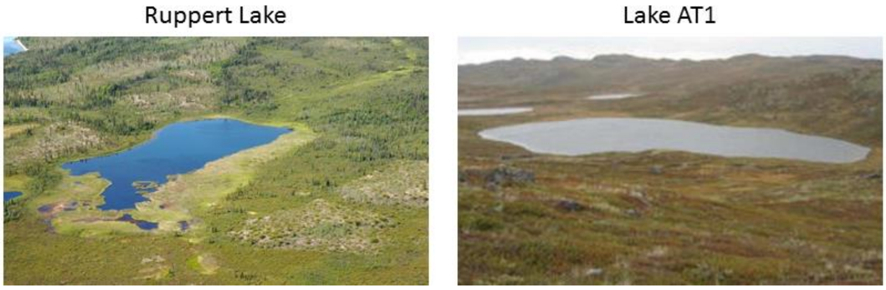

Figure 4. Ruppert Lake and Lake AT1.

2.2 Input Data

2.2.1 Paleolimnological Data: Pollen, Age-Depth Model, Itrax, Carbon Sedimentation Rate

As the aim of this project is to simulate the response of carbon fluxes to changes in catchment vegetation cover as well as climate, the first objective was to identify time periods in which the study lakes were dominated by distinctly different plant functional types (PFTs). Because the LAC project is ongoing, and lake cores taken from Ruppert and AT1 are still undergoing analysis, LAC data was combined with previous paleolimological studies performed at Ruppert and AT1 to meet data needs.

2.2.1.1 Paleolimnological Data from Ruppert Lake

Pervious work performed at Ruppert lake indicated that the site had undergone a number of major shifts in vegetation cover (Higuera *et al.*, 2009, Brubaker *et al.*, 2009). Post deglaciation, the area was dominated by herb tundra until around 13 kyrBP[2] at which point the area experienced an influx of shrub cover, this dominant cover type

[2] kyrBP stands for 'kilo years before present' and indicates thousands of calibrated radio carbon years before 1950.

was followed by a succession of deciduous woodland, ~10.5 kyrBP, a mixed forest-tundra dominate period, 8.5 kyrBP, with the final transition to boreal forest, the vegetation cover type observed today, occurring at 5.5 kyrBP. To avoid the complications of modelling transition periods, it was decided that this project should focus on modelling the catchment and lake during periods at which the system was in equilibrium. These time periods were selected by examining the pollen record produced by Higuera *et al.* (2009). Figure 5 shows the pollen record produced by Higuera *et al*. along with the time slices selected for this study, appearing in red rectangles, namely 2 kyrBP, 6 kyrBP, 7 kyrBP, 9 kyrBP, 11 kyrBP, and 14 kyrBP. The 14 kyrBP time slice is not represented in Higuera *et al*.'s lake core. However, a radio carbon data taken from the base of Ruppert Core B, cored by the LAC project, dates the sediment at 16.7 kyrBP. The composition of herb tundra can be assumed to remain relatively constant and thus the pollen data from 13.5 to 14 kyrBP could be used to approximate its composition.

To calculate the percent PFT cover for the time slices of interest, the pollen counts published in Higuera *et al.* (2009) were digitized from Figure 5 with the use of the ImageJ software package. After the pollen counts were measured they were adjusted to account for differences in pollen productivity according to the method prescribed by Binney *et al.* (2011). Raw pollen counts were divided by the adjustment factors which are displayed in Table 3. The predicted percent cover, based on the pollen counts would be compared with modern percent cover based on remotely sensed data as well as paleo-percent cover modelled by LPJ-GUESS.

Table 3. Pollen productivity adjustment factors proscribed by Binney *et al.* (2011) for the genera found in Ruppert. These adjustment factors were calculated for these species in North America, other studies have estimated the adjustment factor for Europe as the species found in the respective regions differ significantly.

Genera	Pollen Productivity Adjustment Factor	PFT
Picea	1	BNE
Betula	2	IBS
Betula	2	HSS
Alnus	2	HSS
Salix	0.5	HSS
Populus	0.5	IBS
Artemisia	0.5	GFT
Cyperceae	0.5	WetGRS
Poaceae	0.5	GFT

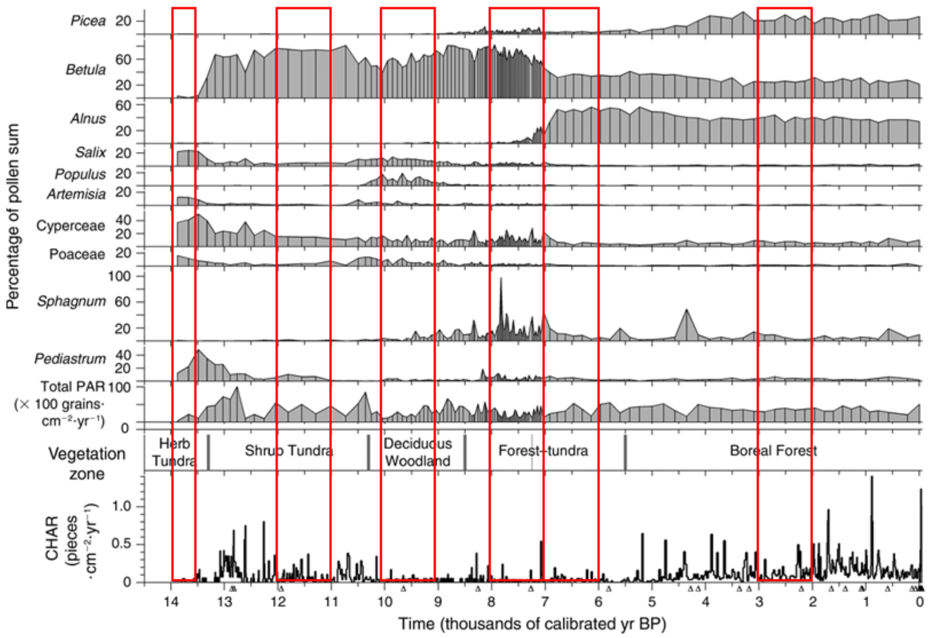

Figure 5. The pollen percentages for Ruppert Lake reproduced from Higuera *et al.* (2009). Time periods used in this study are highlighted with the red boxes.

Two other types of paleo-data, namely carbon sedimentation rate and phosphorus count, were used during the course of this study. Both of these properties were derived from a lake core, Ruppert Lake Core B, taken by Kim Davis from Ruppert during the LAC summer field campaign of 2013. Core B has a total length of 385 cm covering approximately 17,000 years of sediment deposition. Currently two reliable ^{14}C radio carbon dates have been processed for Ruppert Core B. The carbon dates were sent into the NERC Radiocarbon Facility-East Kilbride where they were prepared to graphite and subsequently passed on to the SUERC AMS Laboratory for ^{14}C analysis. The resulting dates were converted from radio carbon years BP to calibrated years BP with software Calib (2 sigma). This processes resulted in the calibrated age of 6,582 ±85 yrBP at a depth of 165.5 cm and a base age of 16,742 ±254 yrBP at 384.5 cm. As two radio carbon dates are insufficient to create an age-depth model for the core, the age-depth model from Higuera *et al.* (2009), seen in Figure 6, was applied to Core B. An age-depth model is a representation of the relation between a sediments age and its depth below the sediment water interface. Such a model is necessary because the rate of sedimentation is not constant through time.

To apply Higuera’s model the sedimentation rate was extracted from a figure published in Higuera *et al.* (2009), shown in Figure 6, via the DigitizeIt software package. An age-depth model was then derived by the LAC core from Ruppert, core B, by assuming the temporal changes in sedimentation rate were relatively the same. The total length of Higuera’s core, 480 cm, is greater than that of Core B. However, at the depth of 165.5 cm, where we have a radio carbon date of 6582 cal yrBP in Core B, Higuera’s age depth model dates that depth at 7250 cal yrBP. Thus, for the depths below 165.5 the sedimentation rate digitized from Higuera was divided by a factor of 1.105, while for depths after 165.5 the sedimentation rate was divided by a factor of 0.546. The sedimentation rate was then applied over time to get the expected age of sediments for given depths. For visualization of the resulting age-depth model the adjustment factors were applied to the radio carbon dates of Higuera *et al.* (2009) (Figure 7).

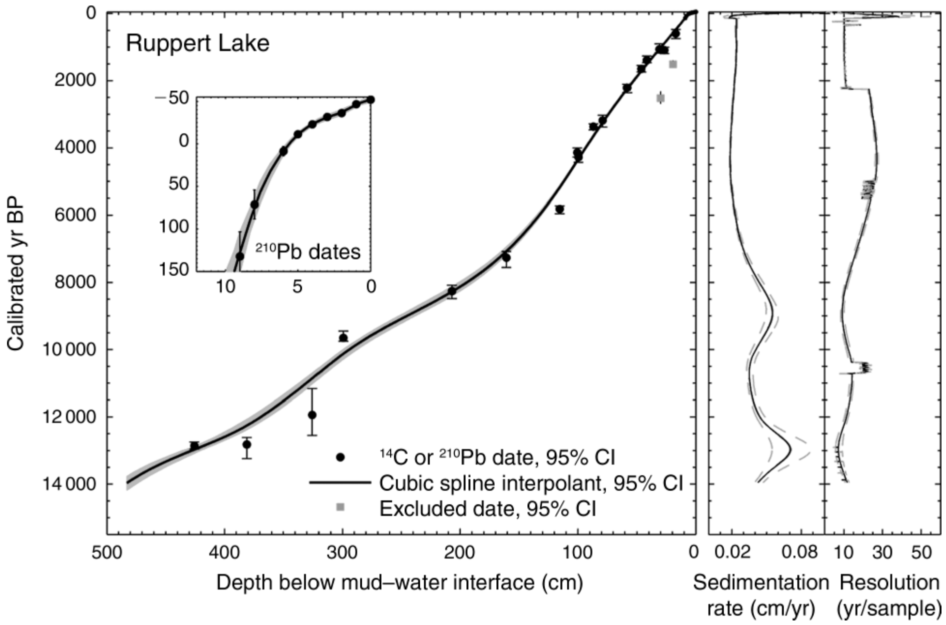

Figure 6. Age-depth model and sedimentation rate for Ruppert Lake reproduced from Higuera *et al.* (2009).

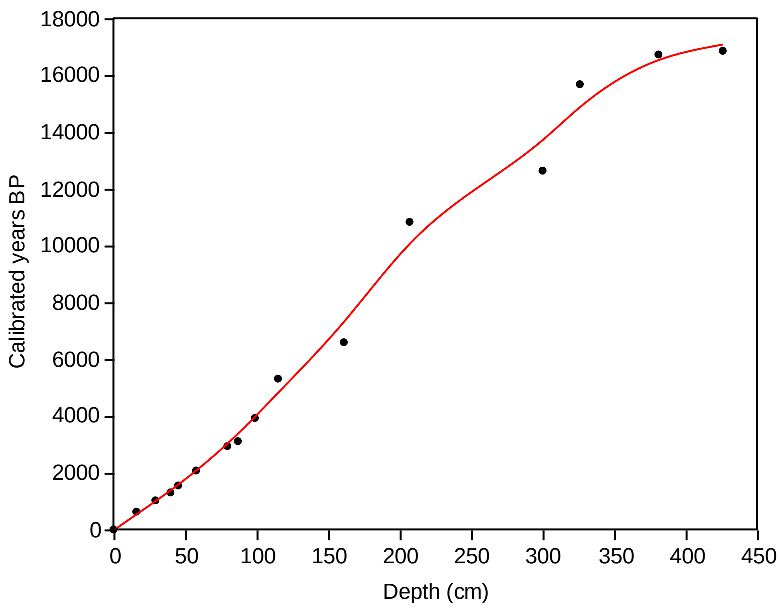

Figure 7. Adjusted age-depth model with points showing the adjusted radio carbon dates from Higuera *et al.* (2009). Visualization was done in this manner to show the effect of the Higuera radio carbon dates on the model.

Once the age-depth model was constructed, Loss On Ignition (LOI) data was used to calculate the carbon sedimentation rate. LOI refers to the weight lost from a sample of sediment after it has been combusted. For Ruppert Core B, LOI was measured by taking 1 cm^2 of sediment every 2 cm of the core. The sediment was dried overnight in a drying oven, and then combusted at 550° C. The resulting LOI data were provided to us by members of the LAC project. To calculate carbon sedimentation from LOI equation 1 was used. The weight lost from a cm^3 sample was divided by 2, to account for the weight of hydrogen and oxygen lost during combustion. It was then multiplied by the sedimentation rate for that particular cm^3 to get carbon sedimentation rate per cm^2. As the lake model output is given in grams carbon entering sediment per square meter per year ($gCyr^{-1}m^{-2}$) the core sedimentation rate was converted accordingly to enable comparison.

$$gCyr^{-1}m^{-2} = (\left(\frac{g}{cm^3}\right)/2) \times (\frac{cm}{yr}) \times 10^4 \tag{1}$$

Paleo-phosphorus data was derived by applying the age depth model to phosphorus counts derived from the Itrax analysis of Core B (Figure 8). The Itrax core scanner is an optical scanning instrument that combines the use of x-ray fluorescence and x-radiography to derive the elemental profiles of sediment cores (Jarvis, 2012). It functions by exposing a continuous sample of the core to x-rays and measuring the radiation the sample reflects. Because different elements reflect unique signals upon exposure to x-rays the Itrax can determine the distribution of an element within the core to sub-millimetre accuracy. The amount of an element is reported in the number of signals corresponding to that element over the total number of signals received called kcps. To determine the concentration of phosphorous, P, within Ruppert for the 1000 year time slices of interest, the average count of each time period, expressed in the units P/kcps, was compared to that occurring in the first 15 cm of the core. According to the age-depth model the first 15 cm correspond to the last 500 years. It was assumed that the accumulation of P within the lake was relatively constant during that time and that changes in P/kcps are proportional to changes in the P concentration within the lake. Because P is a light element and the observed values of P/kcps are barely above the detection limit for the equipment (Jarvis, 2012), zeroes in the data were interpreted as null values and not included in the analysis.

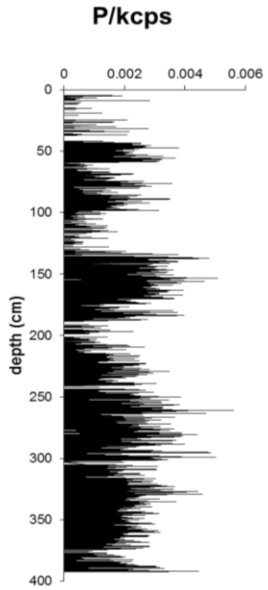

Figure 8. The measured phosphorus counts for Ruppert Core B by the Itrax optical scanner. This data was used to estimate the paleo concentrations of phosphorous within Ruppert Lake.

Paleo-data was also used to derive estimates for lake levels during the specific periods of interest. This was done through the assumption that as these lakes are primarily precipitation fed their levels would vary proportionally in accordance with changes in precipitation reported in Edwards *et al.* (2001).

2.2.1.2 Paleolimnological Date from Lake AT1

The LAC core for Lake AT1 was taken during fieldwork in April of 2014, thus no radio carbon dating, pollen data, or Itrax data for this core have currently been produced. However, because the carbon sedimentation had already been calculated and published in Anderson *et al.* (2012) these values could be compared directly to the coupled LPJ-GUESS/PALM sedimentation values.

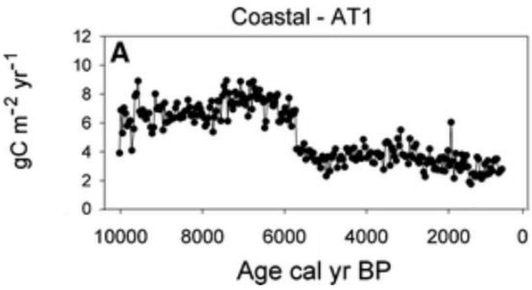

Figure 9. Carbon sedimentation rate calculated for lake AT1 by Anderson *et al.* (2012). Figure reproduced from Anderson *et al.* (2012).

2.2.2 Present Lake and Catchment Characteristics

For this study a number of lake and catchment characteristics are needed including the average depth, catchment area, surface area, and the lakes' ANC and phosphorus content. To calculate Ruppert's mean depth a bathymetry, or topography of the lake floor, was created. Bathymetric measurements and corresponding GPS coordinates were taken by Kim Davis using a Hondex^{TM} Digital Depth Sounder and Garmin GPS in July of 2013 (data used with permission). The collected points were loaded into ArcGIS 10.1 to create a representative TIN for the lake. Two erroneous points were deleted from the bathymetry dataset, point 47 and 73, as they were significantly shallower then the surrounding points and likely created from the sounder detecting aquatic vegetation. From this the average lake depth was calculated for use as input data in the lake model. No bathymetry was created for AT1 instead a reported value for maximum depth and surface was used (Anderson *et al.*, 2012), along with simple geometric assumptions, to calculate mean depth.

Basin area for both lakes was derived from the Advanced Spaceborne Thermal Emission and Reflection Radiometer (ASTER) global digital elevation model (GDEM) which is freely available from the Unites States Geological Survey webportal (http://www.usgs.gov/pubprod/aerial.html#satellite). The ASTER GDEM has a 30 m^2 spatial resolution and is created from stereo-images captured buy the ASTER instrument on the Terra satellite. The ASTER GDEM tends to have anomalies in inland water bodies (Guth, 2010). This is a result of the algorithm being used to create the DEM which does not interoperate the lakes reflectance values as flat surfaces and no post-processing, such as adding lake surfaces to the GDEM from an inland water-body database, has been done (Guth, 2010). Thus, both lakes were manually added through digitizing their surface area and mosaicking the created shapefiles to the ASTER DEM as a flat surface of lower elevation than the surrounding points. The surface area was digitized from images available from Google™ earth specifically a GINA image, acquired 9/13/2008, and a Landsat 8 image, acquired 7/22/2013, for Ruppert Lake and AT1 respectively. The drainage basin, or catchment area, was then derived using a standard function in ArcGIS 10.1.

To derive present day vegetation cover a SPOT 5 image, acquired in July of 2013 and provided by request from the University of Alaska in Fairbanks (http://www.gina.alaska.edu/), was classified into 25 classes the Iso-data unsupervised classification function of ENVI. These classes were then manually reclassified by comparison to aerial photos taken during the 2013 field campaign as well as consultation with a botanist familiar with the site (Edwards, 2013). No SPOT image could be acquired for the AT1 site. Because no aerial photographs were available for AT1, spatial resolution of the satellite images were lower, and the cover types exhibited less distinct spectral profiles Iso-data unsupervised classification was not used on this site. Instead, the NDVI was calculated from a Landsat 7 image, taken during August of 2002. The NDVI values were used to determine the portion of catchment covered by vegetation. The proportions of each PFT were derived from the LPJ-GUESS output.

2.2.3 Climatic Data

Monthly averages for surface temperature, cloud cover, and precipitation, were obtained from the British Atmosphereic Data Center, specifically the Climate Research Unit (CRU) TS 3.21 dataset (http://www.cru.uea.ac.uk/data), which is a 0.5° by 0.5° globally gridded data set covering the period from 1901 to 2012. The CRU dataset proved to be unsuitable for the Alaskan study site due to their proximity to the Brooks mountain range. As Ruppert lies directly at the base of the mountain range, the corresponding CRU grid cell covers areas with higher elevations leading to an underestimation of temperature for the grid cell. For this reason climate data from the nearby Bettles Airport weather station was obtained from the NOAA website (http://www.ncdc.noaa.gov/cdo-web/). CRU cloud cover data were still used for the site as they were not available from the Bettles Airport station.

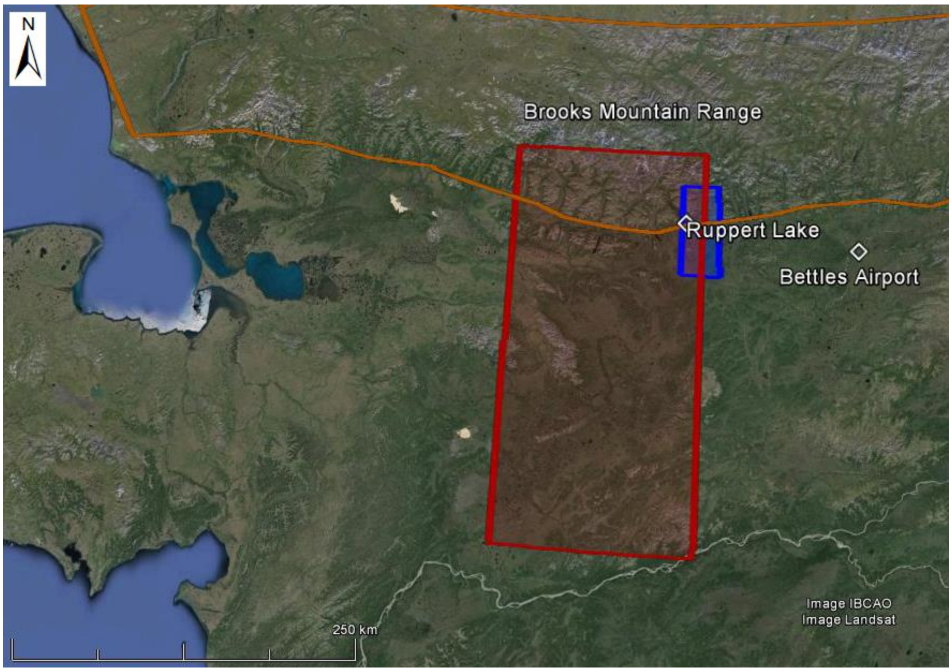

Figure 10. Location of Ruppert Lake in relation to the Brooks Mountain Range and the weather station at Bettles Airport with the CRU, smaller blue rectangle, and HadCM3, larger red rectangle, grid cells. Image taken from Google Earth.

Paleoclimate data was obtained from the Bristol Research Initiative for the Dynamic Global Environment (BRIDGE) research group at the University of Bristol (http://www.bridge.bris.ac.uk/resources/simulations). This research group specializes in testing climate models used to predict global warming by transposing their temporal axis and having them simulate past climate change. The results of these experiments can then be compared to paleo-proxy data in order to evaluate a model's performance. BRIDGE has compiled the results of their work in a database which is accessible upon request.

For this project the climate data produced by Singarayer and Valdes (2010) were used. Singarayer and Valdes used the Hadley Centre climate model (HadCM3), a widely respected global circulation model (GCM) produced by the British Met Office that has been assessed and used by the IPCC (Vavrus *et al.*, 2009), to simulate 'snap-shots' of the average climate for every 1000 years back through 120 kyrBP. Their modelling exercise incorporated climate forcing pressures from changes in orbit, greenhouse gasses, and ice sheet extent. The data is represented as a global grid with spatial resolution of 2.5° latitude by 3.75° longitude over the terrestrial environment. The 'snap-shots' produced by HadCM3 represent the average of modelled 30 year averages for every 1000 year time period. Thus the output is one year of climate data containing monthly averages for precipitation, cloud cover, and temperature that is suitable input for LPJ-GUESS and PALM. This data was downloaded in the form of NetCDFs and the variables of interest were extracted for the study sites with the use of a simple script written in R studio.

The output from HadCM3 was then used to calculate climate anomalies for the 1000 year time periods, or time slices, of interest. Anomalies for precipitation, temperature, and percent cloud cover were derived by taking the difference between the HadCM3 output for the preindustrial era, or 0 kyrBP, and the period of interest for each variable respectively. The climate anomalies were then applied to the modern climate data covering the years from 1952-2012 in order to account for inter-annual climate variation. These adjusted values could then be used as input for PALM and LPJ-GUESS.

2.4 LPJ-GUESS

The Lund-Potsdam-Jena (LPJ)-GUESS is a process based 'gap' model for terrestrial vegetation in which CO_2 and water are exchanged within a modular framework (Smith et al., 2001). LPJ-GUESS uses identical biophysical processes as the DGVM version of LPJ, these principles being derived from the widely known BIOME models (Haxeltine and Prentice, 1996). As a 'gap', or forest dynamic model, a grid cell is divided into non-overlapping patches, with each patch in theory corresponding to the realm of influence of one fully grown individual (Smith, 2001). Generally, a grid cell for LPJ-GUESS is 10 ha comprising of 100 patches, each 0.1 ha in size. The LPJ family of models utilize the plant functional type (PFT) approach to model vegetation. In this approach an "average individual" represents the mean behaviour of a given PFT population, thereby discarding the differences between individual plants and sometimes species to reduce model complexity to a manageable level (Woodward, 1987). Each of these PFTs are defined by their physiology, morphology, phenology, bioclimatic and fire response attributes. The PFTs compete with one another for resources within a grid-cell and each grid-cell is represented by the percent coverage of present PFTs. Grid cells are modelled independently and are scaled to an appropriate size for a given research area. The model begins with bare grid-cells and runs through an initial spin-up phase that allows the vegetation cover to come to equilibrium. Spin-up phases are generally based on a few years of measured data and typically last for 1000 model years. After spin-up, measured historical data is applied to model current ground cover, after which one can apply a scenario phase in which vegetation distribution in the desired climatic scenarios can be modelled (Smith, 2001).

To run LPJ-GUESS one requires monthly average temperature, precipitation, and radiation, the concentration of atmospheric CO_2, and the soil type of the modeled area. With this information the model can produce a variety of output variable including the masses of carbon in the soil and plant material, the net ecosystem exchange (NEE) of carbon, the amount of heterotrophic respiration within the soil, soil moisture, the leaf area index (LAI) of each PFT, and the amount of surface runoff. The basic processes LPJ-GUESS goes through to derive these results are depicted in Figure 11.

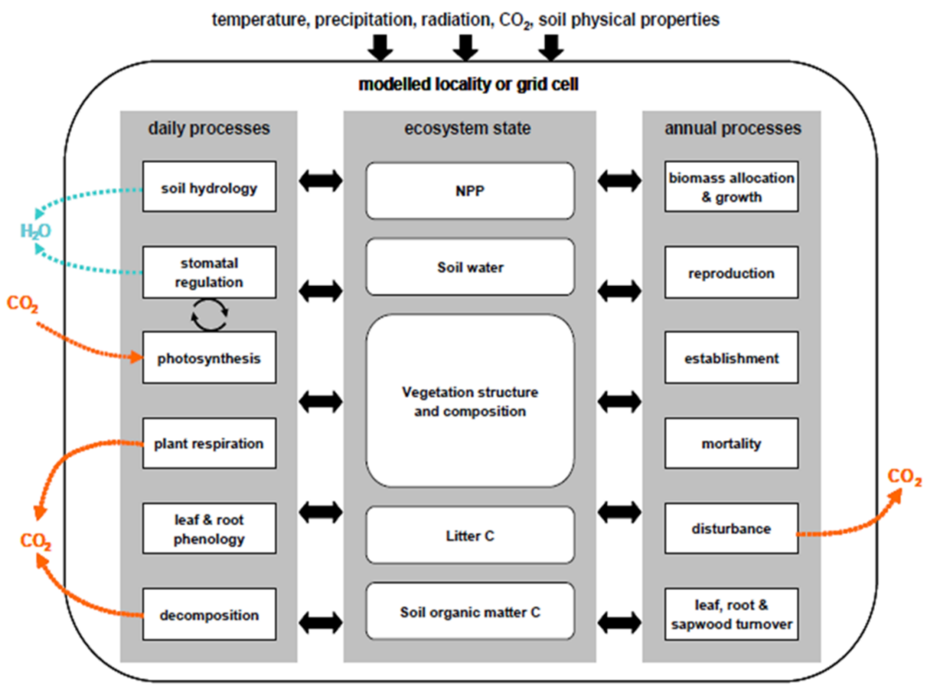

Figure 11. The basic processes undertaken by LPJ-GUESS. Replicated from (Smith, 2001).

2.4.1 Modifications to LPJ-GUESS

The iteration of LPJ-GUESS used for this project is the Miller and Smith (2012) version. This version of LPJ-GUESS uses Arctic specific PFTs, as well as, the modified permafrost and wetland dynamics developed by Wania *et al.* (2009). The subset of PFTs used in this study can be seen in Table 4. The only adjustments made to the defining characteristics of the PFTs was to remove a bioclimatic limit, namely a growing degree day limit called *zero_max*, from the CLM, PDS, and GFT functional types. The source code for LPJ-GUESS, written in the programing language C++, was provided by Paul Miller. To alter the code CMake was used to build the project while the code was altered and compiled with the use of Microsoft Visual C++ Express 2010.

Table 4. PFTs used in this study.

PFT	Designation	Example Genera
BNE	Boreal Shade Tolerant Needle Leaved Evergreens	*Picea*
HSS	Tall Summergreen Shrub	*Betula, Alnus, Salix*
IBS	Boreal Shade Intolerant Broadleaved Summergreen Trees	*Populus, Betula*
GFT	Graminoid and Forb Tundra	*Artemisia, Poaceae*
CLM	Cushion forbs, Lichen, and Moss tundra	*Saxifarage, Dryas, Sphagunum*
WetGRS	Inundation tolerant Grasses	*Carex*
PDS	Prostrate dwarf shrubs	*Salix*
C3G	C3 Grasses	*Poaceae*

2.5 PALM Development

The Paleo-Arctic Lake Model, PALM, was created with the use of MATLAB 2013a. PALM was heavily derived from models produced by Hanson *et al.* (2004) and Cardille *et al.* (2007) that were developed to examine carbon dynamics in temperate lakes. These models were merged and modified based on the available input data and desired outputs.

2.5.1 Hanson et al. 2004 and LUWI

In 2004, Hanson *et al*. created a carbon cycling model to examine how carbon loading affects the balance between autotrophy and heterotrophy within lakes. The model was developed for the Northern Highland Lake District (NHLD) in Michigan. In this model carbon exists in three states: dissolved organic carbon (DOC), particulate organic carbon (POC), and dissolved inorganic carbon (DIC). The export of carbon from the catchment was not explicitly modelled. Loading of carbon into the lake was set to a set of daily values based on the range of DOC observed in the NHLD. Once in the lake, carbon would cycle between its three forms until it is either effluxed, discharged by the outflow, or enters lake sediment. Besides carbon content, the only other water quality variables included in the model are the acid neutralizing capacity (ANC) and the total phosphorus (TP) concentration. From the phosphorus concentration the gross primary production (GPP) within the lake was calculated. While the alkalinity served to determine the fraction of DIC existing as aqueous CO_2. Lake stratification was also included in the Hanson *et al.* (2004) model, with thermocline depth being dependent on the amount of organic matter within the lake (Equation 31).

In 2007, Cardille expanded the work done by Hanson *et al.* (2004) by creating the Lake Uplands/Wetlands Integrator (LUWI) model. (Cardille *et al.*, 2007). The model simulates carbon stocks in the lake catchments, aerial carbon inputs, sedimentation, and atmospheric exchange of carbon, as well as, inter-lake, groundwater, and wetland carbon flows. LUWI derives many of its equations from Hanson *et al*.'s work including those governing GPP and mixing layer depth. One major change LUWI made was not differentiating between the organic carbon stocks within the lake. Instead LUWI combines DOC and POC and represents it all as one carbon stock called simply organic carbon. The major improvements this mode exhibited was the modelling of connections between lakes and the modelling of carbon export from the lakes catchments. LUWI uses a dynamic vegetation model, the Integrated Biosphere Simulator (IBIS), to simulate carbon stocks in the catchment and surface runoff. Another addition made in LUWI was the process of carbon flocculation. Flocculation is the process whereby molecules in a suspension form non-physically bound aggregates and fall out of suspension. This process occurs naturally when the concentration of organic carbon reaches above 40 g m^{-3}. Improvements that the author cited that could be made to LUWI included simulating ice cover, substrate differences along the flow paths, and modelling anaerobic sedimentation. Furthermore, though methane production is indeed an important component of lake carbon cycling it modelled by neither Hanson *et al.* (2004) or LUWI.

2.5.2 Modification and Combination of the Hanson et al. and LUWI Models

To create PALM the processes form the two previous models were combined with some omissions and a few added functions. PALM, like Hanson *et al.* (2004), simulates three carbon pools, DOC, POC and DIC. The equations used to simulated the flow of carbon between these carbon pools are essentially identical to those found in Hanson *et al.* (2004), the only difference being the absence of carbon leaving the lake through outflows and evaporation. PALM also integrates carbon flocculation within the lake from LUWI. The variables and equations governing these flows can be seen in Table 5 and Table 6. Another process that PALM has in common with LUWI is the way in which it simulates runoff from the catchment. Though the vegetation models used are different, the coupled version of PALM also calculates runoff as being the residual of occurring precipitation after evaporation and plant water demand have been deducted. However, PALM does not model changes in lake volume based on the influx of runoff, groundwater, or precipitation. Lake volume is fixed and can only be adjusted manually at the beginning of a run. This means that the model does not model evaporation and outflows, instead for PALM water inflow act as a conveyor of carbon but the water itself does not get added to the lake. PALM also did not incorporate the inter-lake connections from LUWI, but neither of the study lakes had connecting lakes.

The additions to PALM include a more realistic method of representing seasonality, some beneath ice carbon processing, and distinguishing the origin of lake sediment between being derivative of the catchment or being produced within the lake. Both Cardille and Hanson set a fixed number of ice-free days that were split into seasons of a fixed length. PALM took a different approach, allowing the ice free period to vary according to the different temperatures observed each year. In the previous models temperatures within the lake were also fixed for a given season. PALM improved upon this by allowing lake temperatures to vary on a monthly basis, though these monthly values were fixed. To ensure that the lake temperature values corresponded to reasonable values observed within the Arctic, lake temperature datasets were obtained from Toolik Lake, a lake in close proximity to the Ruppert study site, for 1998, 1999, and 2009 (MacIntyre, 2000, Shaver, 2000, Shaver *et al.*, 2011). The average monthly temperature for the combination of these three datasets was written into a file read by PALM. The 1998 data set measured not only changes in surface temperature in Toolik but also measured temperatures throughout the water coulomb. By examining this dataset it evidence for lake stratification was seen when surface temperatures reached 7° C. Therefore, PALM begins to model a stratified lake (Figure 12, C) when its temperature reaches that threshold. Beneath ice processing was represented in PALM in a very simplistic manner by allowing respiration of sediment and deposition of POC to continue during the winter (Figure 12, A).

2.6 PALM Description

After ice break up the lake begins exchanging CO_2 with the atmosphere while receiving carbon from the catchment via runoff, aerial deposition, precipitation and groundwater inflow (Figure 12, B). DIC enters the lake via precipitation, DIC_p, and via ground water. The proportion of DIC in the ground water has been modelled as corresponding to 30 % of incoming catchment DOC (Table 5Table 5). DIC is also produced in the lake through the respiration of the various different carbon pools. DOC enters the lake via catchment runoff, DOC_{in}, and rain water, DOC_p. Once in the lake DOC is slowly respired by heterotrophs (Equations 21-22). As noted previously, during stratification DOC concentration functions to determine mixing layer depth (Equation 31). As the POC enters the lake it slowly settles to the bottom at a rate determined by its average particle size represented by the variable, *pd*, particle diameter (Table 5, Equations 26-29). As the particles settle they are broken down and respired by heterotrophs. This process is expressed in the variable R_{poc} (Equations 23-24). The POC produced by primary production, the allochthonous carbon pool in the lake, is also modelled as planktonic biomass resulting from GPP (Equation 33). This living POC, POC_{EL} and POC_{HL}, dies at a fixed rate and joins the same POC pool as the allochthonous POC. The rate of death rate of the biotic element is higher in the hypolimnion, *hd*, as they are assumed to be intolerant of anaerobic conditions (Table 5). Once in the sediment the organic matter is respired at a low rate for a time (Equation 25) until it is finally sequestered into the sediment permanently.

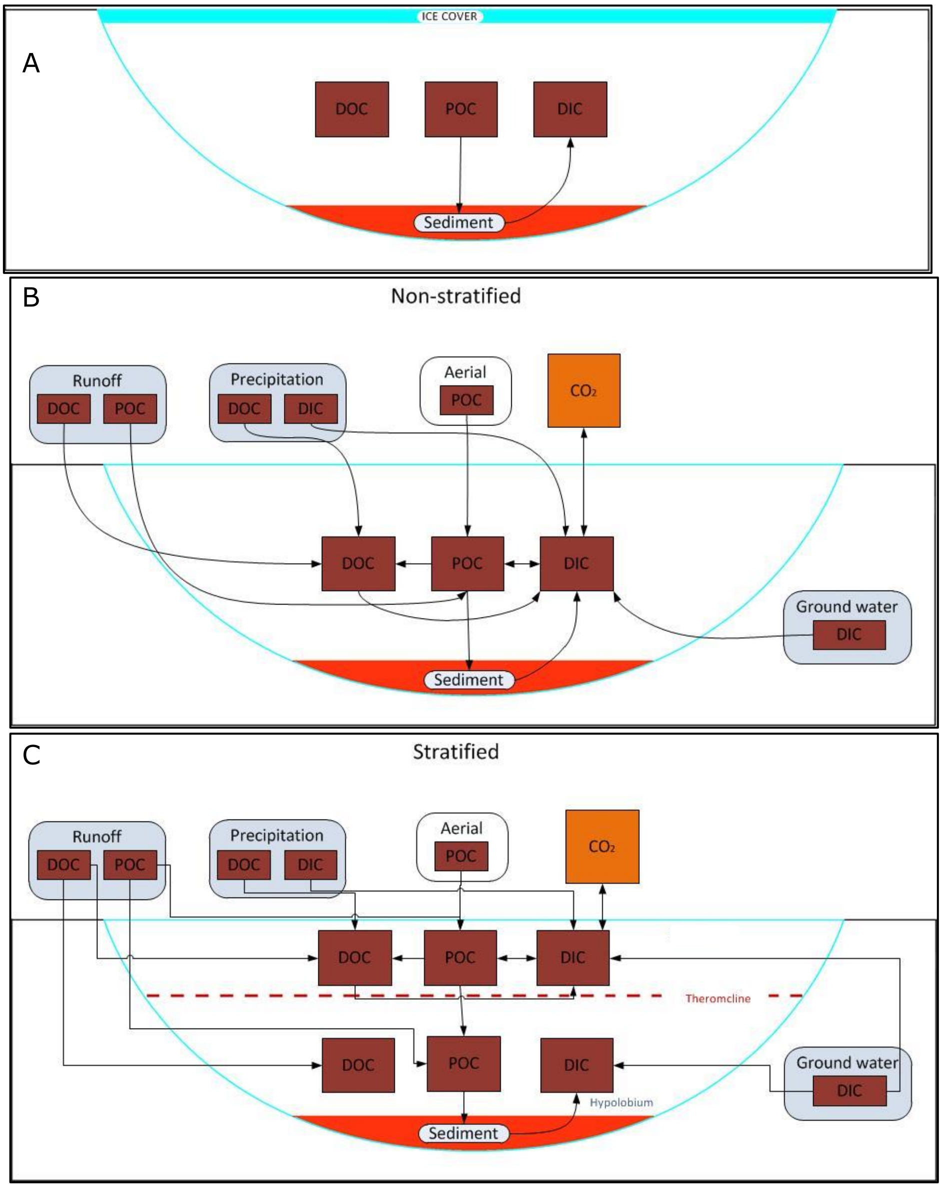

Figure 12. The lake carbon cycle according to PALM. The three lake states are shown along with the major flows of carbon occurring during each period.

Table 5. Variables used in the PALM model, alongside their units, values, and source.

Variable	Variable description	Units	Value	Source
Drivers				
ANC	Acid-neutralizing capacity	μEq L^{-1}		LAC Field Data
ca	Watershed area	m^2		ASTER DEM
d	Mean depth	m		*lv/la*
DIC_{in}	DIC loading from groundwater	g m^{-3}	0.3 DOC_{in}	
DIC_p	DIC loading precipitation	g m^{-3}	1 x *p*	Willey et al. (2000)
DOC_{in}	DOC loading from surface water	g m^{-3}		Look Up Table (Table 7)
DOC_p	DOC precipitation	g m^{-3}	2 x *p*	Willey (2000)
POC_{air}	Aerial POC loading	g m^{-2}		Look Up Table (Table 8)
POC_{in}	POC loading from surface water	g m^{-3}		Look Up Table (Table 8)
la	Lake surface area	m^2		LAC Field Data
lv	Lake volume	m^3		LAC Field Data
RU	Surface runoff	mm m^{-2} day^{-1}		LPJ-GUESS
p	Precipitation	mm day^{-1}		NOAA/CRU
TP	Total Phosphorus	μgL^{-1}		LAC Field Data/CRU
Constants				
a	GPP that becomes exudate	Proportion	0.030	Biddanda & Benner (1997)
ed	Death of algae rate constant (epi)	day^{-1}	0.030	Connolly & Coffin (1995)
ef	Conversion of POC to DIC	day^{-1}	0.050	Hanson (2004)

	(epi)			
eg	Conversion of DOC to DIC (epi)	day^{-1}	0.005	Houser (2001)
hd	Death of algae (hypo)	day^{-1}	0.900	Hanson (2004)
hf	Conversion of POC to DIC (hypo)	day^{-1}	0.050	Hanson (2004)
hg	Conversion of DOC to DIC (hypo)	day^{-1}	0.005	Hanson (2004)
kCO_2	Efflux of CO_2 piston velocity	$m\ day^{-1}$	0.500	Cole et al. (2002)
pd	Diameter of particles	µm	5.000	Wetzel (2001)
ra	GPP that is respired	Proportion	0.800	Quay et al. (1986); Cole et al. (2002)
Lake state variables				
DIC	Dissolved inorganic carbon	$g\ C\ m^{-3}$		Output
DOC	Dissolved organic carbon	$g\ C\ m^{-3}$		Output
efflux	Respiration	$g\ C\ m^{-3}\ day^{-1}$		Output
GPP	Gross primary production	$g\ C\ m^{-3} day^{-1}$		Hanson et al. (2003)
POC_D	Dead POC	$g\ C\ m^{-3}$		Output
POC_L	Living POC	$g\ C\ m^{-3}$		Output
Sed	Sediments	$g\ C\ m^{-3}$		Output
zmix	Thermocline depth	m		Snucins & Gunn (2000)

Table 6. Equations governing Carbon cycling in PALM.

Carbon transport to the lake:

$$DOC_{in} = \frac{RU \times caDOC \times ca}{lv} \quad (2)$$

$$POC_{in} = \frac{(POC_{air} \times la) + (RU \times caPOC \times ca)}{lv} \quad (3)$$

$$DIC_p = (1 \times p) \quad (4)$$

$$DOC_p = (2 \times p) \quad (5)$$

Carbon Dynamics Epilimnion:

$$DOC_E = DOC_{in} + DOC_p + GPP_{ex} - R_{doce} \quad (6)$$

$$POC_{EL} = GPP - RA - GPP_{ex} - Sed_{EL} - Death_{EL} \quad (7)$$

$$POC_{ED} = POC_{in} + Death_{EL} - R_{poce} - Sed_{ED} \quad (8)$$

$$DIC_E = 0.3 \times DOC_{in} + RA + R_{poce} + R_{doce} + RS - GPP - efflux \quad (9)$$

Sedimentation and Efflux:

$$Sed = Sed_{EL} + Sed_{ED} + C_{floc} - R_s \text{ (Non-stratified)} \quad (10)$$

$$Sed = Sed_{HL} + Sed_{HD} + C_{floc} - R_s \text{ (Stratified)} \quad (11)$$

$$efflux = KCO_2 \times \left(CO_{2_{aq}} - CO_{2_{atm}}\right) \quad (12)$$

Carbon dynamics in the Hypolimnium:

$$DOC_H = DOC_{in} - R_{doch} \quad (13)$$

$$DIC_H = 0.3DOC_{in} + R_s \quad (14)$$

$$POC_{HL} = Sed_{EL} - Death_{HL} - Sed_{HL} \quad (15)$$

$$POC_{HD} = POC_{in} + Sed_{ED} + Death_{HL} - Sed_{HD} - R_{poch} \quad (16)$$

Intermediate equations:

$$CO_{2_{atm}} = \left(\frac{1}{8.205\times10^{-5}\times(T_{air}+273.15)}\right)\times\left(\frac{[CO_2]\times12}{10^6}\right) \tag{17}$$

$$CO_{2_{aq}} = 12\times\left((2\times DIC_E)-ANC\right)\times\left(\frac{\left(\frac{-9866}{T_{lake}+273.15}\right)+24.12}{1000}+1\right) \tag{18}$$

$$RA = GPP\ \times ra \tag{19}$$

$$GPP_{ex} = GPP\times a \tag{20}$$

$$R_{doce} = DOC_E\ \times eg \tag{21}$$

$$R_{docn} = DOC_E\ \times hg \tag{22}$$

$$R_{poce} = POC_{ED}\ \times ef \tag{23}$$

$$R_{poch} = POC_{HD}\ \times hf \tag{24}$$

$$R_s = Sed\times sf \tag{25}$$

$$Sed_{EL} = POC_{EL}\ \times 0.0188\times\left(\frac{\left(\frac{pd}{2}\right)^2}{d}\right) \tag{26}$$

$$Sed_{HL} = POC_{HL}\ \times 0.0188\times\left(\frac{\left(\frac{pd}{2}\right)^2}{d}\right) \tag{27}$$

$$Sed_{ED} = POC_{ED}\ \times 0.0188\times\left(\frac{\left(\frac{pd}{2}\right)^2}{d}\right) \tag{28}$$

$$Sed_{HD} = POC_{HD}\ \times 0.0188\times\left(\frac{\left(\frac{pd}{2}\right)^2}{d}\right) \tag{29}$$

$$Death_{EL} = POC_{EL}\times ed \tag{30}$$

$$Death_{HL} = POC_{HL}\times hd \tag{31}$$

$$\ln(zmix) = -0.739\times ln([OC])+2.698 \tag{32}$$

$$GPP = 0.012\times\exp(0.883ln(TP)) \tag{33}$$

$$\text{If } [OC]>40:\ C_{floc} = [OC]-40\left(\frac{[OC]}{20+[OC]}\right) \tag{34}$$

2.6.1 Sensitivity Analysis and Model Validation

To determine which components of PALM made the greatest impact on carbon sedimentation and efflux a sensitivity analysis was performed. This was performed by increasing each variable in PALM by 10% and comparing the resulting annual sedimentation and efflux to a baseline value. This baseline value for sedimentation and efflux was obtained by running PALM for Ruppert Lake with averages calculated from the 1952-2013 NOAA precipitation and temperature data and the average runoff modelled by LPJ-GUESS for the present time period. The average value of total phosphorus, alkalinity, and DOC were taken from a dataset extracted from the Long Term Ecological Research Network (LTER) to serve as baseline values for the sensitivity analysis. This particular dataset contains biogeochemical information collected during the period between 1988 and 2010 for ground water, streams, and lakes located in the lake rich area north of the Brooks Mountain Range (Kling, 2013). There are over 2000 measurements of ground water and streams in this data set and over 600 lake measurements. Not all of these measurements contain values for POC, DOC, phosphorus, and ANC, but the dataset is extensive and gives a good idea of the range of values occurring within the region. Two other variable ranges, namely that of piston velocity, KCO_2, and aerial particulate deposition, POC_{air}, were added to the model validation utilizing ranges reported in the literature. The average annual sedimentation and efflux were taken from the 21st year of each run, after the model had reached equilibrium. Validation of the model was done by forcing it to run under the most extreme conditions observed in the LTER dataset and cited by the literature and assessing if the output remained reasonable.

Table 7. Baseline for the sensitivity analysis is shown alongside the maximum and minimum values found in the cited sources.

	TP (ug/L)	ANC (meq/L)	DOC (mg/L)	caPOC (mg/L)	KCO_2 (k600)	POC_{air} (g m^{-2} day^{-1})
Baseline	15.91	1.325	16.13	0.34	0.5	0.0385
Max.	135.05	3.286	40	8.695	0.75	0.056
Min.	0.93	0.16	2.04	0	0.35	0.021
Source	LTER	LTER	LTER	LTER	(Cole *et al.* 2010)	(Carpter *et al*. 2005)

2.7 Coupling PALM to LPJ-GUESS

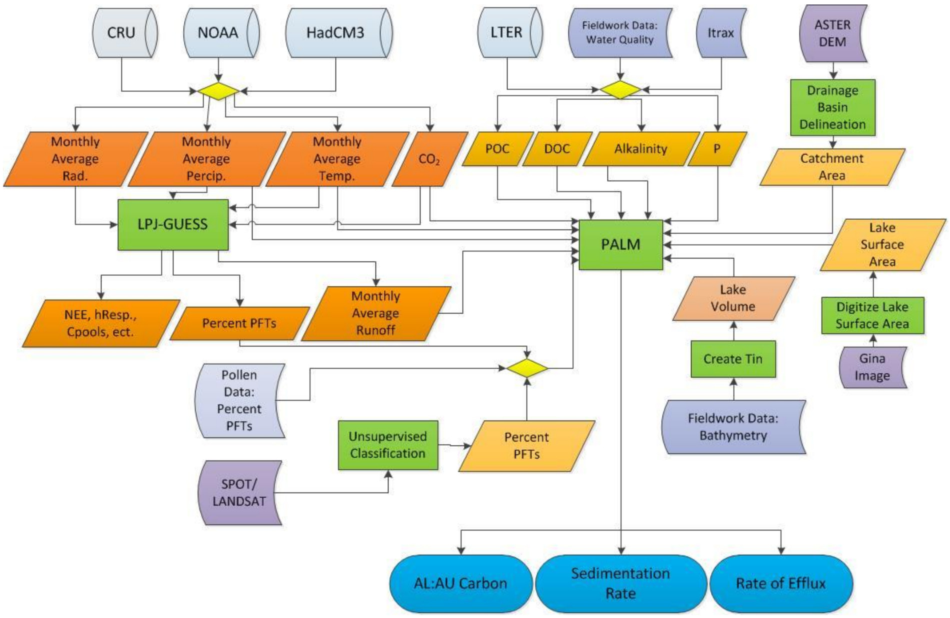

Figure 13. Methodology used during the course of this work showing input databases and data sources, the needed input data for the models, and the resulting outputs.

Once both models were functional and the input data was collected, the experiments examining the impact of vegetation cover and climate change were carried out. To derive the necessary runoff data for PALM, LPJ-GUESS was run on the modern and paleo climate data. As the project aims to simulate the catchment/lake system at equilibrium LPJ-GUESS was set up so that for each period it would use detrended data, i.e. the order of input climate data was randomized, for each time slice, namely present day, 2 kyrBP, 6 kyrBP, 7 kyrBP, 9 kyrBP, 11 kyrBP and 14 kyrBP, to spin-up for 1000 years and then apply the trended data as the experimental run. Only 57 of the 60 years of input data were used for Ruppert Lake as the climate data collected from Bettels weather station had missing values for the period between 2001 and 2003. These years were also removed from the climate data corresponding to site AT1 in order to achieve consistency throughout the runs. Outliers were not removed from the climate data as they represented natural variation which was desirable. The output files contained the last 57 years of the detrended spin-up period and the 57 years of trended data. Though all standard outputs for LPJ-GUESS were produced, the variables of interest for this experiment were the yearly output of carbon stocks, variable name *cpools*, monthly runoff, *mrunoff*, and the LAI, *lai*. Monthly runoff, while not increasing the volume of the lake, did determine the amount of DOC and POC entering the lake. The *cpool* data was used to approximante the concentration of POC in the monthly runoff. Finally, LAI was used to quantify the percent catchment cover of each PFT. LAI was converted to catchment cover with the standard equation (35) developed by (Sitch *et al.*, 2003) where FPC, or fractional percent cover, is expressed in values from 0 to 1.

$$FPC_{PFT} = 1 - \exp(-0.5 LAI_{PFT}) \qquad (35)$$

To run PALM with the monthly output values from LPJ-GUESS the amount of monthly runoff was simply divided by the number of days in each month. To set up the experimental run PALM was run for 20 years on then averaged climate and runoff input values for each time slice. The model was the allowed to run for 57 years of available input data. Depending on the run different sources were used as input data.

The quantity of DOC and POC coming off of the catchment was derived by equations 2 and 3. The concentration of DOC produced in runoff by each PFT type was taken from the literature (Table 8). The concentration of POC in the runoff was made to be proportional to the average amount of each PFT entering leaf litter as simulated by LPJ-GUESS. The highest contributor to the leaf litter, BNE, was set to have a POC concentration of 1 g m^{-3} for its runoff, this value is based the range of dissolved POC concentrations observed in the LTER (Kling, 2013) dataset. Precipitation input was also formatted as a monthly average, thus the DOC and DIC derived from that source was added at a corresponding constant rate for each month based on concentrations reported in Willey *et al.* (2000). Aerial POC input is wholly based on the proportion of PFTs present in a time slice and is added at a daily rate during the ice free period. The amount of aerial POC input was derived by combining the range of aerial deposition reported in Buffam *et al.* (2011), namely 0.0560-0.0210 g m^{-2} of lake surface area, with information on the pollen productivity of each PFT (Table 3).

Table 8. Look-up table used to determine the concentration of DOC within upland runoff contributed by each PFT type. Here *N* represents the number of observations the value is based on and σ the standard deviation.

Covertype	DOC (g m^{-3})	*N*	σ	Sources
BNE	36.9	41	23.0	Aitkenhead-Peterson *et al*. (2002)
CLM	1	1	NA	Koprivnjak & Moore (1992)
HSS, PDS	31.0	3	24.5	Neff *et al*. (2002); Koprivnjak & Moore (1992)
IBS	27.4	14	10.2	Aitkenhead-Peterson *et al*. (2002)
WetGRS	37.7	4	11.5	Aitkenhead-Peterson *et al*. (2002)
GFT, C3 grass	7.2	2	2.9	Aitkenhead-Peterson *et al*. (2002)

Table 9. Look-up table used to calculate concentration of POC contributed by each PFT.

PFT	caPOC (g m^{-3})	POC_{air} (g m^{-2})
BNE	1.0000	0.0385
CLM	0.9116	0.0210
GFT, C3G	0.7821	0.0210
IBS	0.8287	0.0560
HSS, PDS	0.7646	0.0560
WetGRS	0.8287	0.0210

Results and Analysis

3.1 PALM: Sensitivity and Validation

Table 10 reveals the effects of the different variables in PALM on carbon sedimentation and efflux. The maximum increase of sedimentation, 9.75 %, is shown when lake temperature is increased by 10 %. This can be attributed to longer growing periods for the primary producers, a longer ice free period where POC deposition occurs, and increased lake stratification which decreases the amount of POC respired by bacteria before it enters the sediment. Increasing particle diameter, *pd*, increased sedimentation by 9.4 %. This increase is likely caused by the reduction of time spent in the water column and the resulting decrease in respiration. Aerial input of POC also seems to be a large contributor to sedimentation as increases in *airPOC* and lake surface area, *la*, also both showed a 6.09 % positive increase in sedimentation. Increases in *caPOC*, catchment area, and the volume of runoff also had a small positive effect on sedimentation but they were minor, only 2.87 %, in comparison. Increasing lake volume had the greatest negative effect on sediment deposition. Increasing lake volume and lake depth both increase the time POC spends in the water column and were shown to have a relatively large negative effect on sedimentation. Increasing the respiration rate of POC and GPP also had a notable negative effect. Lake temperature followed by the respiration rate of GPP had the greatest positive effect on CO_2 efflux. Lake temperature is likely so influential because it directly impacts the proportion of aqueous CO_2 (Table 6, Equation 17).Though these effects are not simulated in PALM, in reality the temperature of the water would also prolong the ice free period and the amount respiration occurring in the lake. The amount of DOC loading from the catchment was also shown to be a very influential in affecting carbon efflux. This is evidenced by the substantial increase of around 10 % in efflux due to increases in *caDOC*, catchment area, and runoff, *RU*. The dilution of the lake caused the most significant drop in efflux, ~11 %, seen in the effect of increasing *lv*, lake volume. The fixing of DIC through GPP also lessened efflux, but only by ~ 3 %. A small negative effect, -1.68 %, was also seen by increasing particle diameter, which indicates that the respiration of POC does contribute slightly to CO_2 efflux.

Table 10. PALM variables were increased by 10% to determine their effect on the amount of carbon efflux and sedimentation. The percent change in annual sedimentation and efflux resulting from the 10% increase in each variable is shown in columns 3 and 4 of this table.

Variable	Sedimentation (%Δ)	Efflux (%Δ)	Variable discription
a	-0.18	0.56	GPP to DOC conversion rate
ANC	0	0	Alkalinity
ca	2.87	11.30	Catchment area
caDOC	0	10.63	Concentration of DOC runoff
caPOC	2.87	0.67	Concentration of POC runoff
CO2	0	-0.00228	Atmospheric CO2 concentration
d	-4.58	0.85	Average lake depth
ed	0.44	0.04	Death rate of algae (ep)
ef	-3.27	0.92	POC to respiration rate (ep)
eg	0	-0.01	DOC to respiration rate (ep)
GPP	1.04	-3.15	Gross primary production
hd	-0.0033	0.00023	Death rate of algae (hyp)
hf	-1.30	-0.08	POC to respiration rate (hyp)
hg	0	-0.15	DOC to respiration rate (hyp)
kCO2	0	-0.00182	Piston velocity at k600
la	6.09	1.32	Lake surface area
lv	-8.15	-11.48	Lake volume
pd	9.40	-1.68	Average particle diameter
POCair	6.09	1.32	Aerial input of POC
POCin	8.96	1.99	Combine aerial and runoff POC
precip	0	0.52	Precipitation on lake surface
ra	-4.87	14.81	Respiration rate of GPP
RU	2.87	11.30	Runoff from catchment
sf	-0.63	0.16	Sediment to DIC conversion rate
T	0	-0.00205	Air temperature
temp	9.75	17.13	Lake temperature
TP	0.80	-2.42	Total phosphorus
zmix	0	0	Thermocline depth

The results of the sensitivity analysis were used to test if PALM would respond realistically to extreme conditions. This was performed by running the model with the set of conditions found in Table 7 that would either maximize or minimize sedimentation or efflux. The subsequent sedimentation and efflux values are seen in Table 11. The resulting sedimentation and efflux rates fall within the range of values reported for boreal lakes in the literature (Table 12).

Table 11. Efflux and sedimentation resulting from PALM being run with the baseline input data as well as the most extreme values it can produce for Ruppert Lake given the range of cited literature data in

	Efflux (g m^{-2} yr^{-1})	Sed. (g m^{-2} yr^{-1})
Baseline	14.3	2.3
Max.	40.3	7.0
Min.	-11.1	1.1

Table 12. A selection of reported literature values for sedimentation and efflux from studies done in the Arctic.

Literature Values (g m^{-2} yr^{-1})		
Efflux	Sedimentation	Reference
25 -39	14-39	(Buffam *et al*. 2011)
2	2.3	(Christensen *et al*. 2007)
4.5	0	(Jonsson *et al*. 2007)
-84	NA	(Pacheco *et al*. 2013)

To further solidify the assertion that modelled carbon fluxes in Ruppert Lake are realistic the model's output for a number of years for the "present day" time slice are shown herein (Figure 14). These years were selected because they are sequential and show a large degree of variability, which will served to demonstrate the model's response to changing conditions. The fluxes not only follow a reasonably realistic pattern but the measured DOC concentration observed in Ruppert during the 2013 field campaign, namely 8.39 g m^{-3}, falls within the 1-17 g m^{-3} range of concentrations observed during these years.

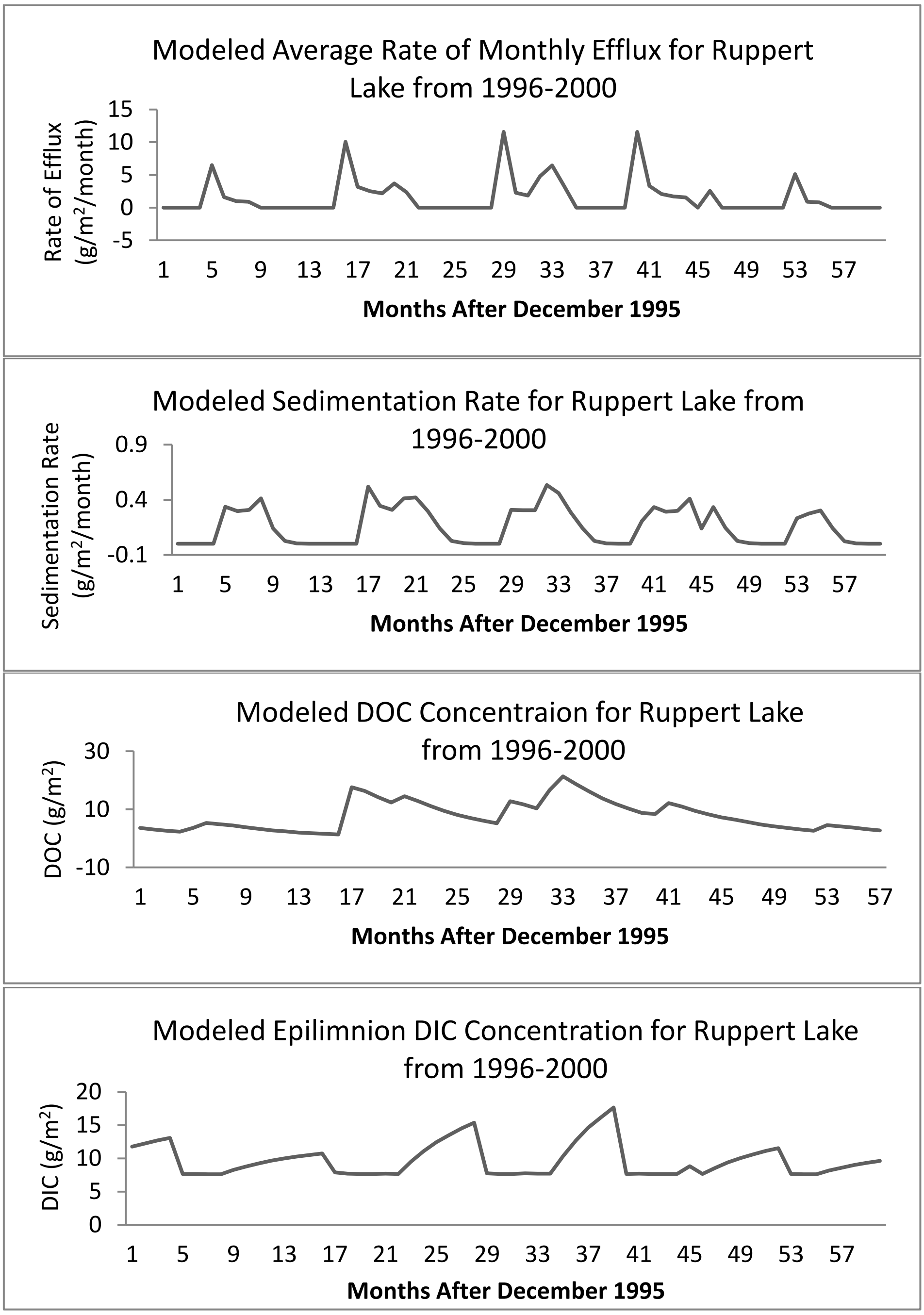

Figure 14. Carbon fluxes modelled for Ruppert Lake by the linked version of PALM and LPJ-GUESS for the years 1996 to 2000. Climate input data used for these runs are from Bettles Airport, Alaska, and P and ANC taken from field data collected in 2013.

3.2 Catchment PFT Cover

The method used to derive catchment area in this study did not account for inflowing streams in either study cite. In essence, because the lake model was not constructed so that it could account for stream inflows and outflows for the purposes of this study the AT1 and Ruppert were modelled as seepage, lakes with no streams entering or exiting, and not drainage lakes. Therefore, their catchment area is underestimated which can be seen from the fact that the catchment area for AT1, derived using ArcGIS 10.1, was much smaller than the value reported by the literature. This issue was not rectified because the extent and path of the incoming stream was unknown. Therefore, for the coupled runs of PALM, the catchment area delineated by ArcGIS 10.1 was used. The catchment area measured in this study for Ruppert was ~ 40 ha while that of AT1 was ~ 50 ha. AT1's reported catchment size in the literature is 150 ha (Anderson *et al.*, 2012).

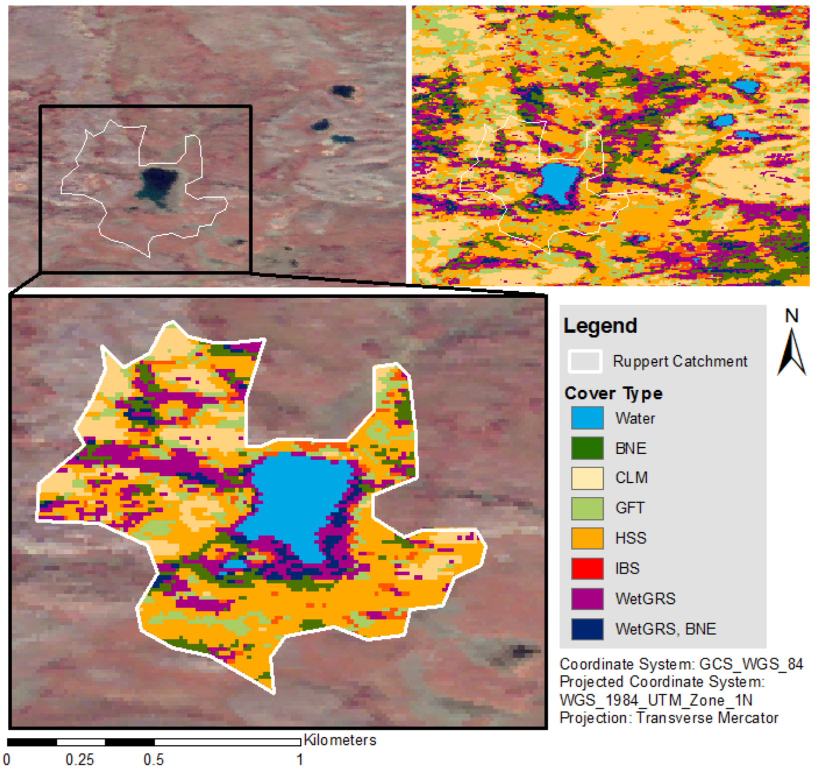

Figure 15. (A) SPOT 5 image used for the unsupervised classification is displayed as a standard false colour composite with the catchment being calculated in ArcGIS displayed as a white polygon. (B) The PFT classification

derived from the SPOT image. (C) A close-up of the classified catchment with corresponding scale bar.

To determine the validity of modelled LPJ-GUESS percent PFT cover a comparison dataset was constructed using satellite image classification, and a classification based on the pollen record in Ruppert Lake. The percent PFTs in Figure 15 do not correspond directly to the calculated pollen percent results. One modification was made to the pollen percent results, namely the addition of 12 % of the CLM PFT for each paleo time slice, i.e. 2 kyrBP to 14 kyrBP. This was done based on the 12 % CLM vegetation cover observed in the SPOT classification. The species in the CLM cover type either do not produce pollen or do not produce it in a manner that would contribute to a pollen record found in lake sediment. Because this cover type occupies the exposed moraine tops this area is likely to have been occupied by the CLM cover type since lake formation. This is evidenced by the lack of top soil witnessed in these areas during field work. For, these reasons the CLM percent cover was added to the rest of the pollen predicted percent covers in order to make the cross validation with LPJ-GUESS, which models CLM, to be more realistic. Furthermore, the percent cover of *Sphagnum* is displayed separately from the other cover types as its spore counts cannot quantified in the same manner as the other pollen counts. It is shown because it can be used as a relative indicator of moisture within the catchment (Edwards, 2013).

The results of the satellite image classification produce percent PFT covers typical for a boreal forest (Figure 15, A), which corresponds well to the PFT covers produced from the pollen data for both the 0 kyrBP and 2 kyrBP time slice (Figure 15, B). The small underrepresentation of BNE, which are exemplified in Ruppert's catchment by *Picea* spp., can be attributed to the fact that the forest is still in the process of regrowth due to a fire in the area in 1991 (http://fire.ak.blm.gov/predsvcs /maps.php).

The modelled results from LPJ-GUESS do not correspond well to either the satellite observed percent PFTs or the results derived from the pollen data. As can be seen in Figure 16, C, the BNE PFT is overly dominate when present, 0 kyrBP to 7 kyrBP, and in general LPJ-GUESS fails to display the reasonable proportions of PFTs, always allowing one PFT to dominate the catchment. Moreover, the results displayed in Figure 16, B, were achieved only by including the PFTs that were expected for a given time period to be present for that run. This was done by manually editing the program code to exclude the other PFTs modelled by LPJ-GUESS from the runs. When LPJ-GUESS was run with all PFTs represented PFTs such as BSN, or boreal summer-green needle leaved trees exemplified by the genera *Larix*, were modelled in the catchment. The LPJ-GUESS run with all PFTs included did, however, show some catchment vegetation cover trends that matched with observations in the pollen data. For example, the BNE PFT did become less prevalent after 9 kyrBP. However, on a whole this method of applying LPJ-GUESS on the Ruppert catchment failed to give realistic PFT cover, necessitating the approach that led to the results shown in Figure 16. Because the land cover classification based on the pollen data was deemed more realistic, these predicted percent covers along with the values reported in Table 8 and Table 9 were used to calculate the expected concentration of POC and DOC in catchment runoff, as well as the expected aerial input of POC, for each time period of interest. The resulting concentrations are displayed in Table 13 and were used to run PALM during the time periods of interest.

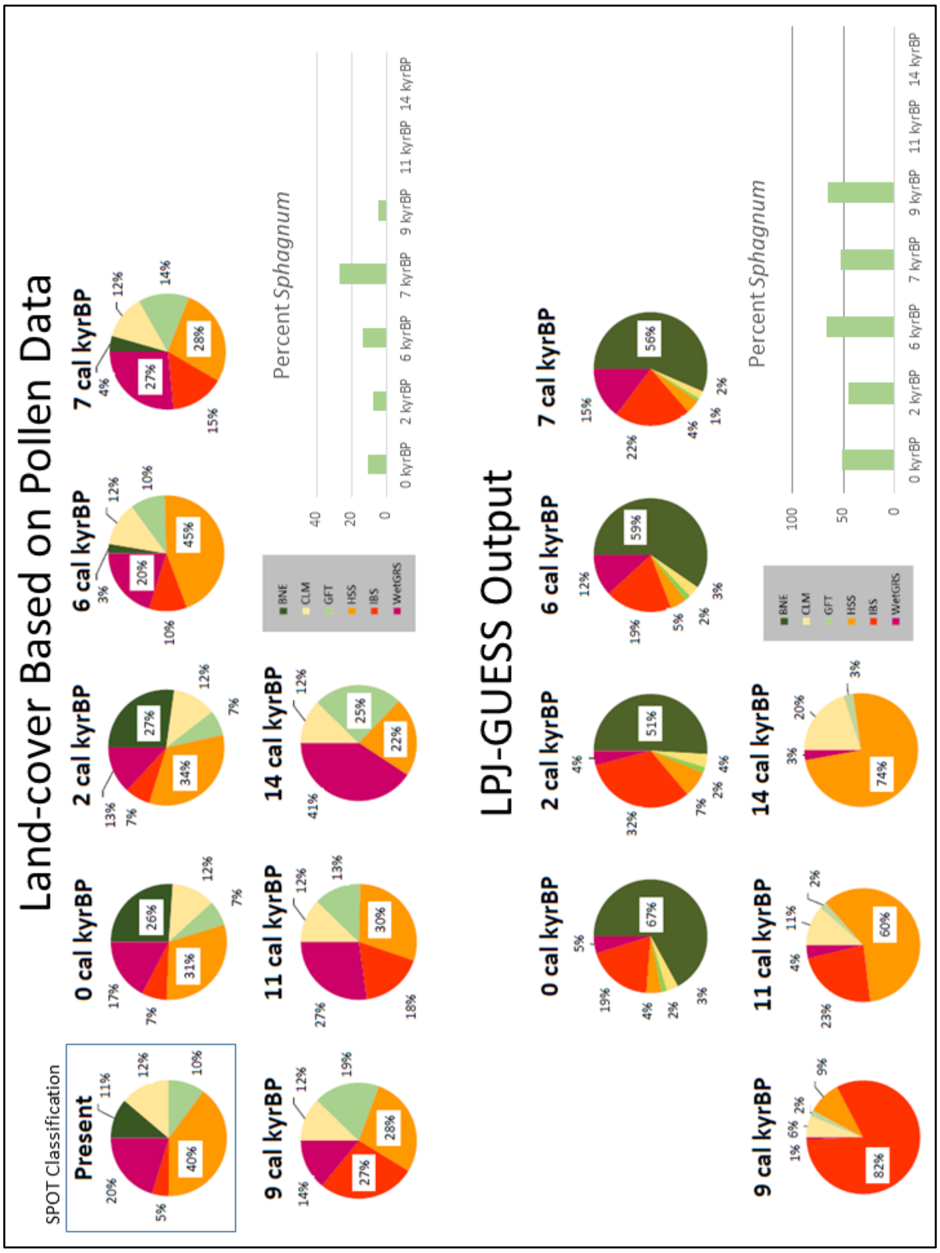

Figure 16. PFT percent cover derived from various sources for Ruppert Lake's catchment.

The same method of only allowing expected PFTs used in Ruppert was applied for lake AT1 resulting in the percent PFT covers for the time slices of interest shown in Figure 17. LPJ-GUESS did simulate herb dominated tundra in 9 kyrBP and significant amounts of prostrate dwarf shrubs for the 2 kyrBP and present day time slice. However, this was only accomplished by again manually excluding other competing PFTs.

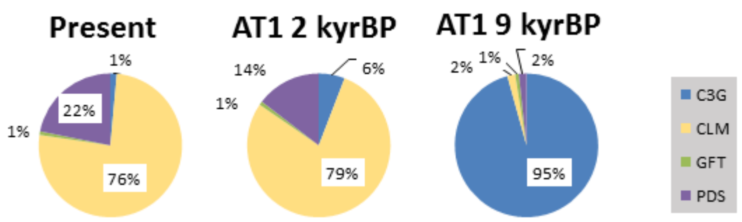

Figure 17. PFT cover modelled for the catchment of AT1 by LPJ-GEUSS.

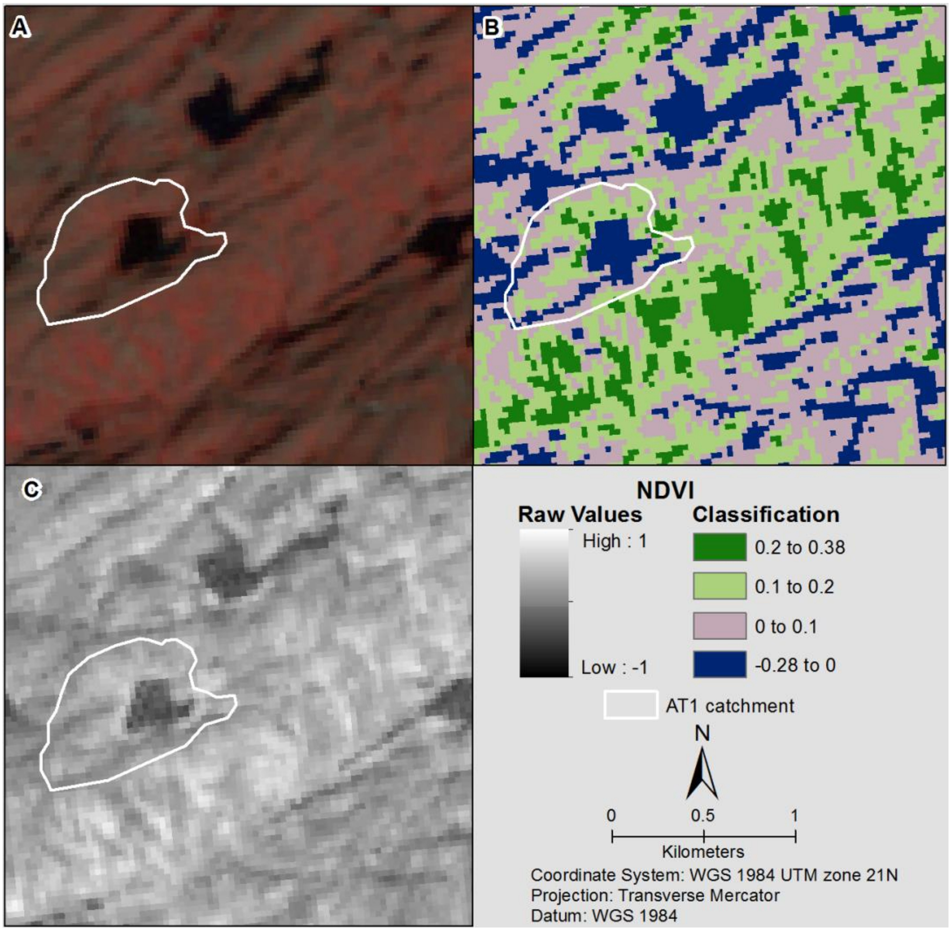

Figure 18. Images of Lake AT1 and the surrounding area, with catchment calculated by ArcGIS displayed as a white outline. (A) Landsat 7 shown as a standard false colour composite. (B) Classified NDVI image of the area where classes are thought to correspond to moderately dense vegetation, 0.2-0.3 , light vegetation, 0.1-0.2, exposed soil, 0.1-0, and wet areas, below 0. (C) NDVI image, calculated from the Landsat 7 image, which was classified.

Due to a lack of images with sufficient resolution and lack of knowledge regarding current ground cover, no attempt was made to classify PFTs cover percent with satellite data. Instead the proportion of PFTs in AT1 was based on the proportions of PFTs calculated by LPJ-GUESS (Figure 17). However, as the catchment is known to contain large areas of exposed bedrock (Liversidge, 2012), NDVI was calculated to determine the area within the catchment that is vegetated. Within AT1's catchment 46% of the area had an NDVI of more than 0.1 and was deemed to be vegetated (Figure 18). Exposed bedrock was assumed not to contribute to runoff POC or DOC. Based on the PFT percent covers calculated by LPJ-GUESS the concentration of POC and DOC coming off of the catchment via runoff was calculated for each time slice and used as input parameters for PALM. These calculated concentrations can be seen in Table 13.

Table 13. Concentrations of incoming carbon calculated for the different time periods for Ruppert Lake and Lake AT1.

Time	*caDOC* (g/m^3)	*caPOC* (g/m^3)	*POCair* (g/m^2)
Ruppert Lake			
Present	25.03	0.852	0.039
2 kyrBP	26.93	0.878	0.040
6 kyrBP	24.92	0.832	0.041
7 kyrBP	24.75	0.823	0.036
9 kyrBP	22.86	0.813	0.040
11 kyrBP	24.93	0.821	0.038
14 kyrBP	23.11	0.820	0.028
Lake AT1			
Present	6.93	0.891	0.029
2 kyrBP	5.39	0.890	0.026
9 kyrBP	7.48	0.786	0.022

3.3 Paleo-conditions in Ruppert

Analysis of the Itrax data showed significantly different phosphorus counts for the time periods of interest (Figure 19, A) despite the fact that all the values had overlapping standard deviations (Figure 19, B). As previously noted, the variation observed in sediment counts was assumed to be proportional to variation between the time periods of TP concentration in the lake. These predicted TP values along with the calculated values for changes in lake surface area, *la*, and lake volume, *lv*, can be seen in Table 14.

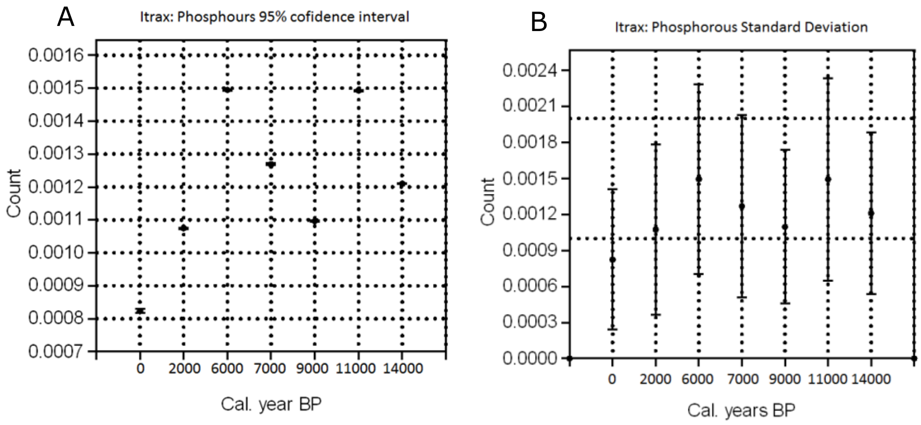

Figure 19. The mean and 95% confidence intervals from the Itrax phosphorus count data (A) alongside the standard deviation observed within the said data (B) for the time period of interest.

Table 14. Percent change in precipitation assumed by this study, based on reported literature values (Edwards *et al.*, 2001) that were used to adjust volume and surface area for Ruppert Lake. The resulting volumes and surface areas, along with the *TP* values which are based on the Itrax counts, are shown.

Time	Precip. (Δ%)	*lv* (m^3)	*sa* (m^2)	*TP* (ug/L)
Present	0	78500	37400	3.46
2 kyrBP	10	86350	41140	4.52
6 kyrBP	0	78500	37400	6.28
7 kyrBP	0	78500	37400	5.33
9 kyrBP	-5	74575	35530	4.61
11 kyrBP	-20	62800	29920	6.28
14 kyrBP	-40	47100	22440	5.09

3.4 Modelled vs. Measured Sedimentation Rates

3.4.1 Ruppert Lake

The organic matter sedimentation rate observed in Ruppert Core B shows a significant amount of variation through time (Figure 20). The variation observed for the time periods of interest are seen in Figure 21, A. When compared to the modelled output seen in Figure 21, B, though the magnitude of sedimentation is underestimated by an order of magnitude for all but the 14 kyrBP time slice, the pattern of variation is strikingly similar. In cases, 9 kyrBP and 14 kyrBP shows means significantly different from almost all of the other time periods (Table 15) with 9 kyrBP having the highest mean and 14 kyrBP the lowest.

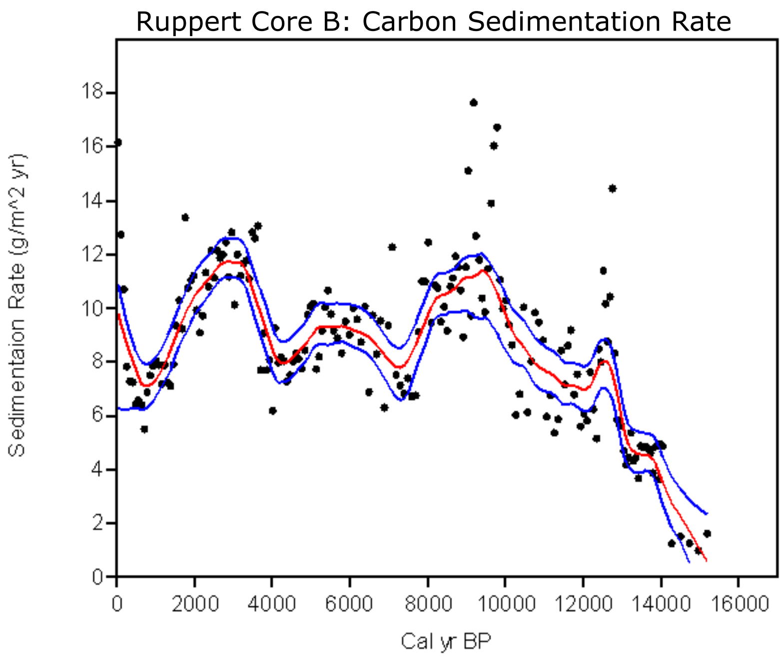

Figure 20. Organic matter sedimentation observed in Ruppert Lake, Core B. The red line is a LEOSS smoothing spline applied with a smoothing factor of 0.3, while the flanking blue lines showing the 95% confidence interval.

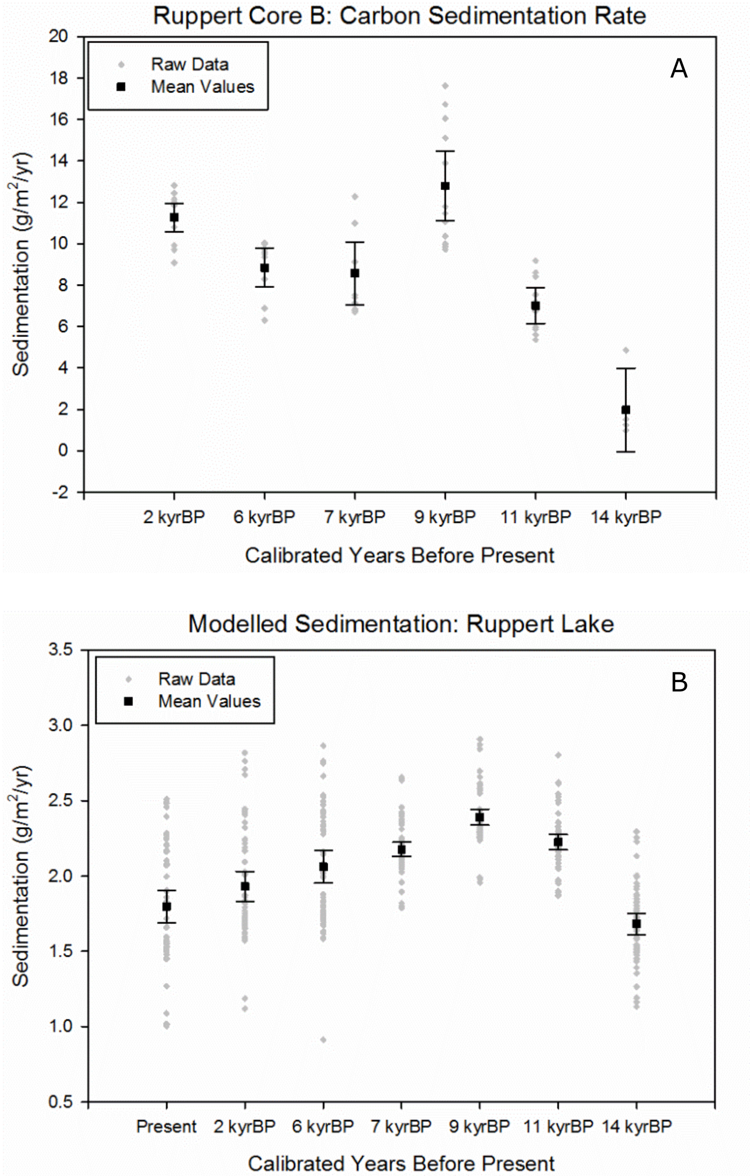

Figure 21. Sedimentation observed in Ruppert Core B is compared to the coupled output of LPJ-GUESS and PALM run under different conditions. Grey dimonds show the distribution of annual sediment accumulation, while the black boxes indicated the mean and the bars show the 95% confidence derived from a non-paired students T-Test. (A) The sedimentation observed within Ruppert Core B. (B) Experimental run of the coupled PALM model where lake volume, runoff, incoming carbon concentrations, and phosphorus were varied.

Table 15. Results of an unpaired students T-test, preformed in the R statistical package, comparing the mean sedimentation rates observed from the coupled PALM output. Significant differences are highlighted in red while marginally significant differences are highlighted in yellow.

Modelled Sedimentation Ruppert						
P-values	Present	2 kyrBP	6 kyrBP	7 kyrBP	9 kyrBP	11 kyrBP
2 kyrBP	0.072					
6 kyrBP	0.001	0.079				
7 kyrBP	0.000	0.000	0.054			
9 kyrBP	0.000	0.000	0.000	0.000		
11 kyrBP	0.000	0.000	0.008	0.180	0.000	
14 kyrBP	0.072	0.000	0.000	0.000	0.000	0.000

Another set of experiments was run with the coupled version of PALM to parse out the drivers behind the differences in observed sedimentation rate. Four more model runs for each time slice were carried out, where all variables, except for the variable of interest, was kept at present day values. Lake volume, phosphorus, runoff, and carbon concentration were all independently varied. The results of this experiment, seen in Figure 22 and Figure 23, seem to indicate that variation in runoff and carbon concentration are the major contributors to the observed trend in Figure 21, B.

To determine whether allochthonous or autochthonous carbon was the major carbon source entering sediment the average ratio of allochthonous to autochthonous sediments, AL:AU, was calculated for Ruppert Lake. In all time slices autochthonous heavily dominated in its contribution to sedimentation (Table 16).

Table 16. Ratios of allochthonous or autochthonous in Ruppert Lake during the time slices of interest.

Time	Present	2 kyrBP	6 kyrBP	7 kyrBP	9 kyrBP	11 kyrBP	14 kyrBP
AL:AU	0.0268	0.0284	0.0300	0.0265	0.0238	0.0282	0.0298

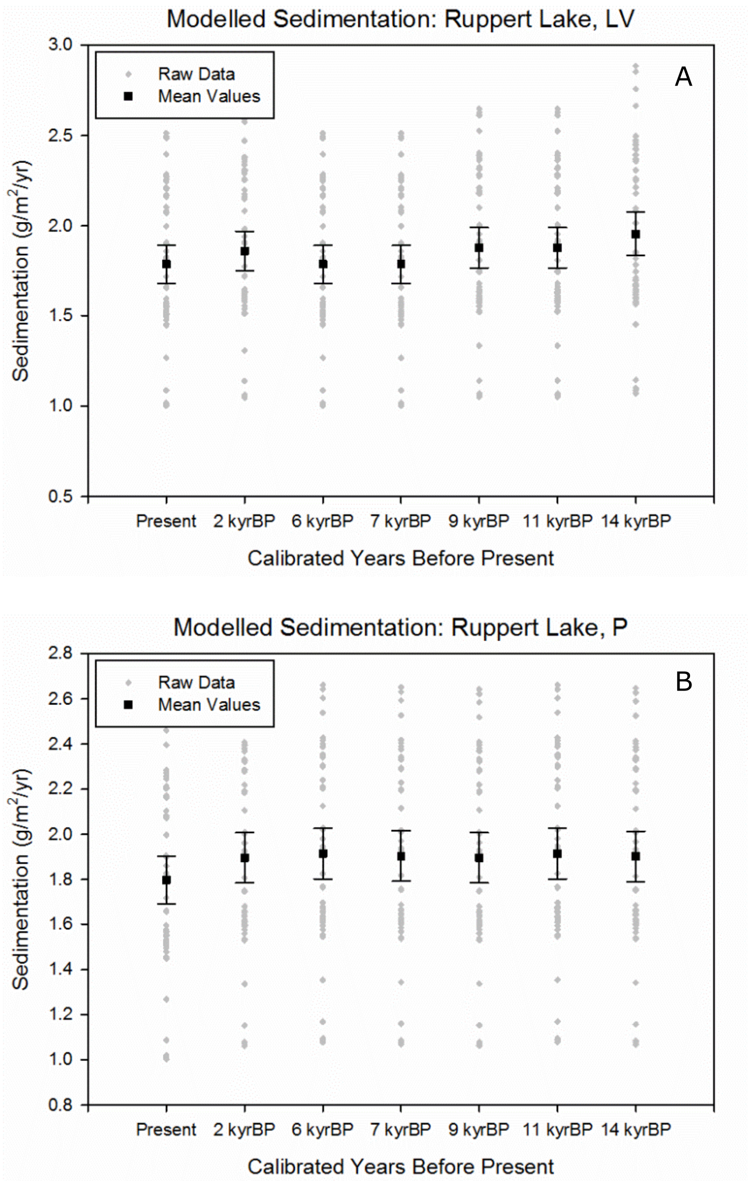

Figure 22. Modelled rate of carbon sedimentation by the coupled version of PALM. The second experimental run set all model inputs to the present time except for a variable of interest. (A) The resulting sedimentation rates from varying catchment lake volume and surface area. (B) The resulting sedimentation rates from varying concentration of phosphours.

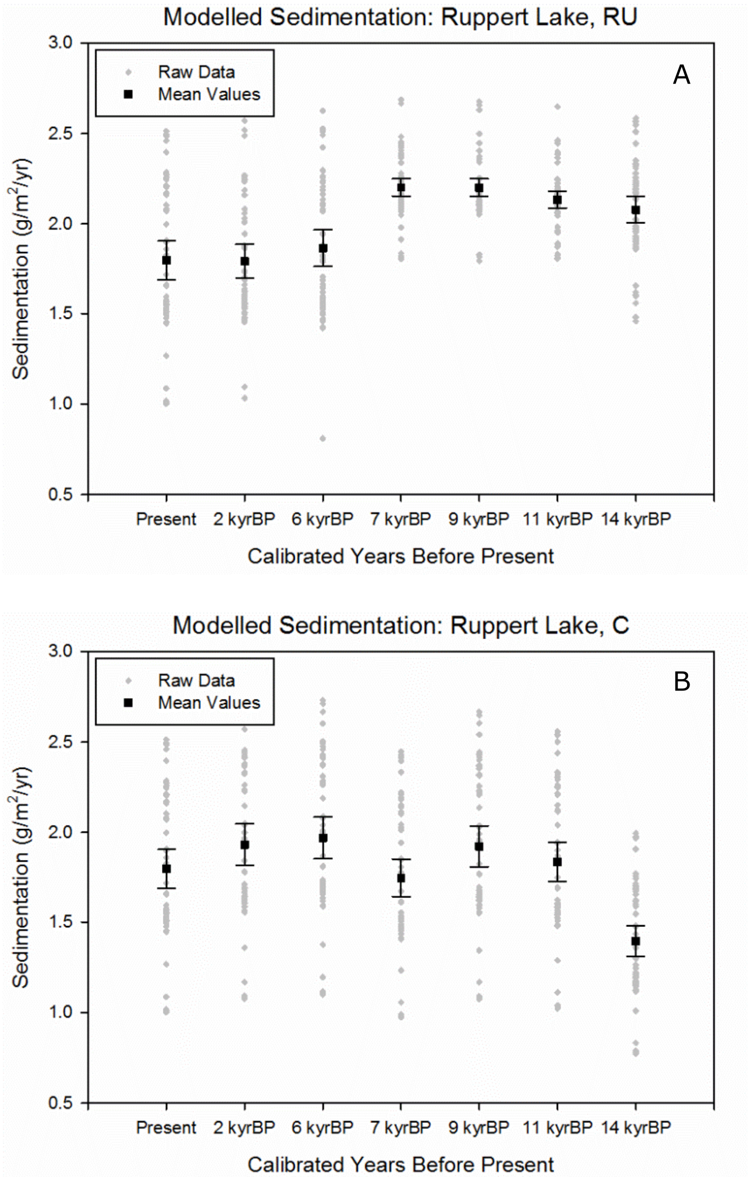

Figure 23. Modelled rate of carbon sedimentation by the coupled version of PALM. The second experimental run set all model inputs to the present time except for a variable of interest. (A) The resulting sedimentation rates from varying catchment runoff. (B) The resulting sedimentation rates from varying concentrations of carbon in runoff and rate of aerial deposition.

The efflux for the coupled model was also analysed to observe how efflux from Ruppert Lake might vary between the time slices (Figure 24). The observed values for efflux were of a reasonable magnitude; however, there are no paleolimnological estimates with which to compare them. Moreover, the modelled effluxes showed less significant differences than the sedimentation rates (Table 17). For the second experiment, the observed changes in efflux seemed to be most driven by lake level change and differences in runoff (Figure 25 and Figure 26).

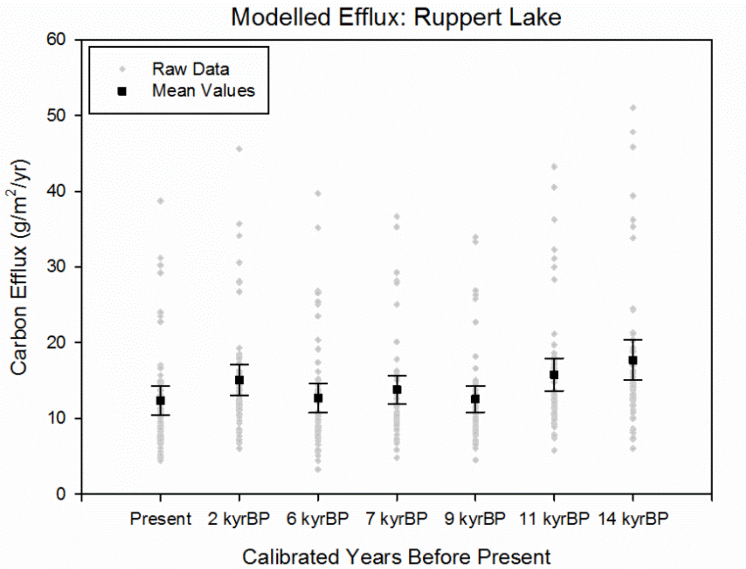

Figure 24. Modelled rate of CO_2 efflux by the coupled version of PALM for the time slices of interest.

Table 17. Results of an unpaired students T-test, preformed in the R statistical package, comparing the mean efflux rates observed from the coupled PALM output. Significant differences are highlighted in red while marginally significant differences are highlighted in yellow

Modelled Efflux Ruppert Lake						
P-values	Present	2 kyrBP	6 kyrBP	7 kyrBP	9 kyrBP	11 kyrBP
2 kyrBP	0.055					
6 kyrBP	0.840	0.089				
7 kyrBP	0.302	0.344	0.415			
9 kyrBP	0.877	0.065	0.954	0.357		
11 kyrBP	0.018	0.616	0.031	0.151	0.021	
14 kyrBP	0.001	0.114	0.003	0.016	0.002	0.261

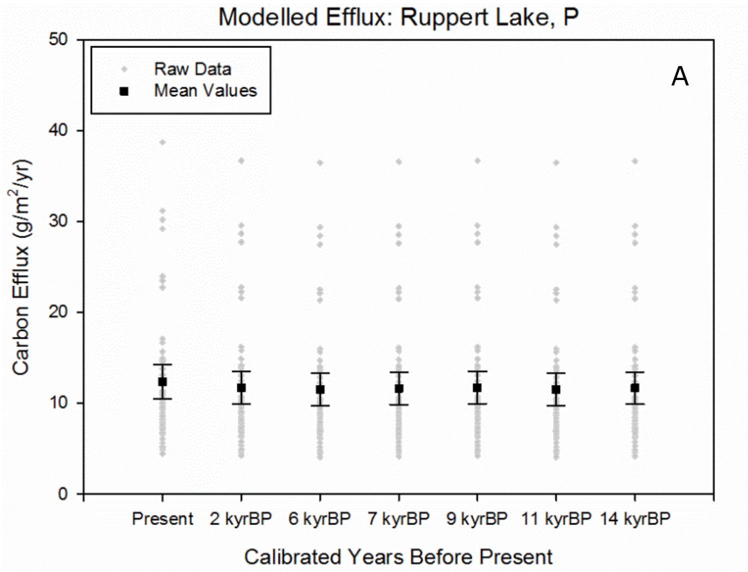

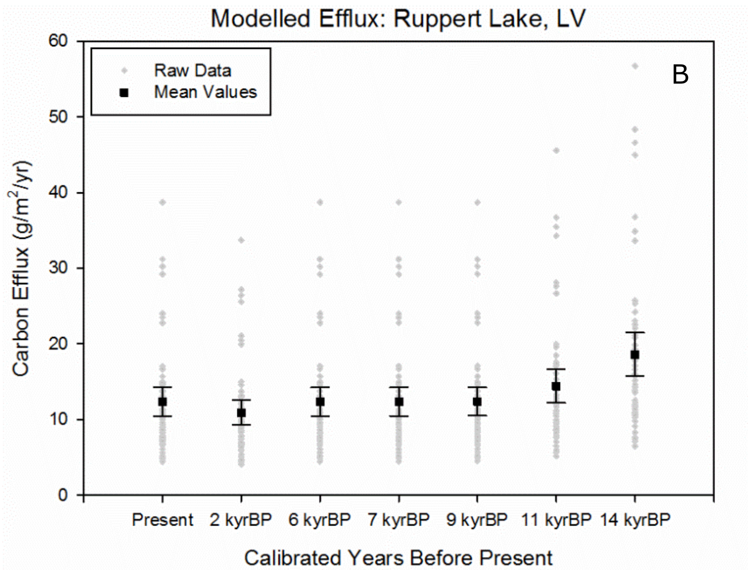

Figure 25. Modelled rate of CO_2 efflux by the coupled version of PALM for the second experimental run in which all inputs were set to model the present time except for a variable of interest. (A) The resulting efflux rates from varying phosphours. (B) The resulting efflux rates from varying and surface area.

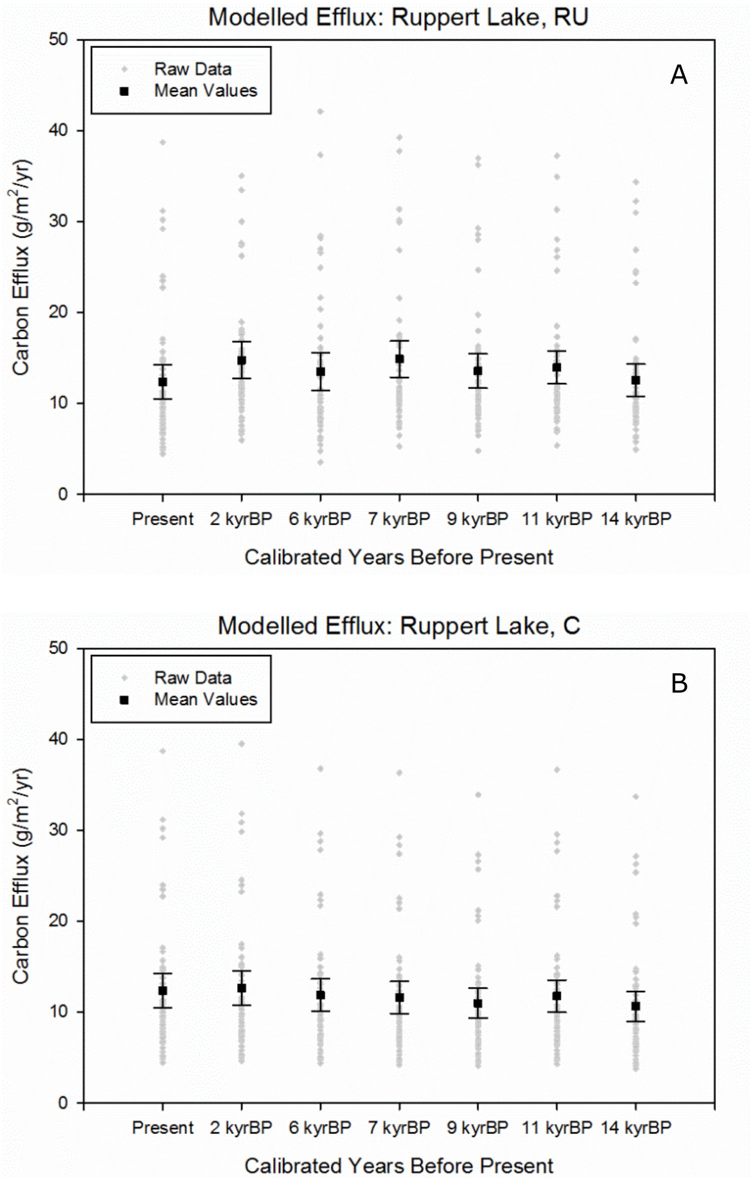

Figure 26. Modelled rate of CO_2 efflux by the coupled version of PALM for the second experimental run in which all inputs were set to model the present time except for a variable of interest. (A) The resulting efflux rates from varying catchment runoff. (B) The resulting efflux rates from varying concentrations of carbon in runoff and rate of aerial deposition.

3.4.2 Lake AT1

The results from Lake AT1 have some interesting facets. For one, the sedimentation rate is again an order of magnitude less than the observed rate in the sediment core. However, for Lake AT1 the pattern of modelled sedimentation is the reverse of paleolimnological observations. Furthermore, sedimentation for the present day is also significantly different from that in 2 kyrBP, a pattern again not observed in the lake core (Figure 27). The modelled effluxes are also of interest as they show much higher modern rates of CO_2 efflux and that in some years for both 2 kyrBP and 9 kyrBP. Moreover, the lake is shown to be a net carbon sink for some years for both 2kyrBP and 9kyrBP (Figure 28).

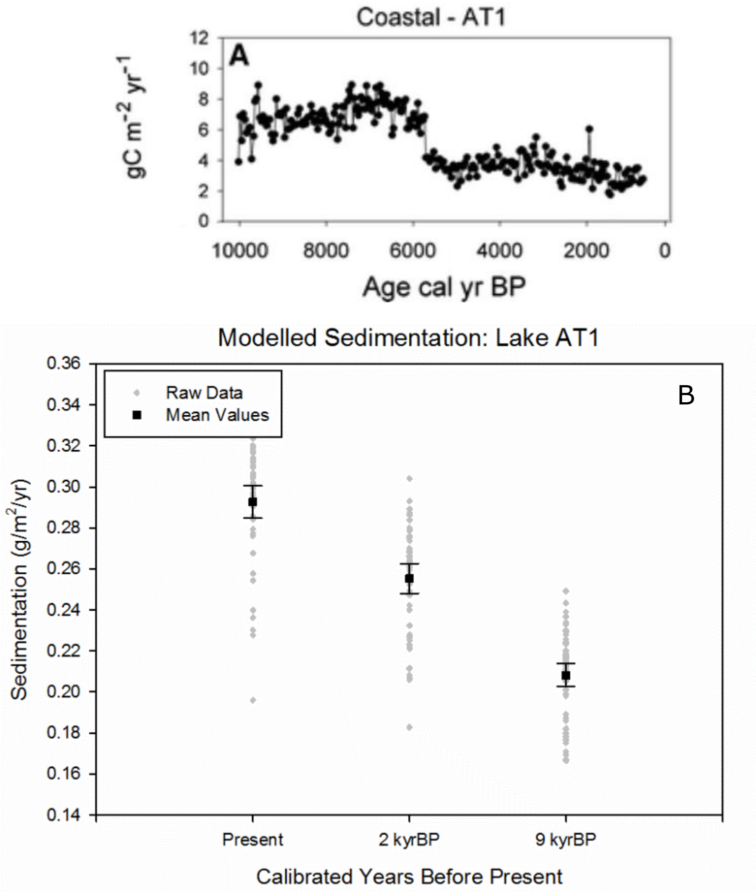

Figure 27. (A) Carbon sedimentation rate calculated for lake AT1 by Anderson *et al.* (2012). Figure reproduced from Anderson *et al.* (2012). Note that Anderson's temporal axis is reversed in comparison to the figures shown in this project. (B) Modelling results from the coupled version of PALM showing sedimentation rate in AT1 for the time slices of interest.

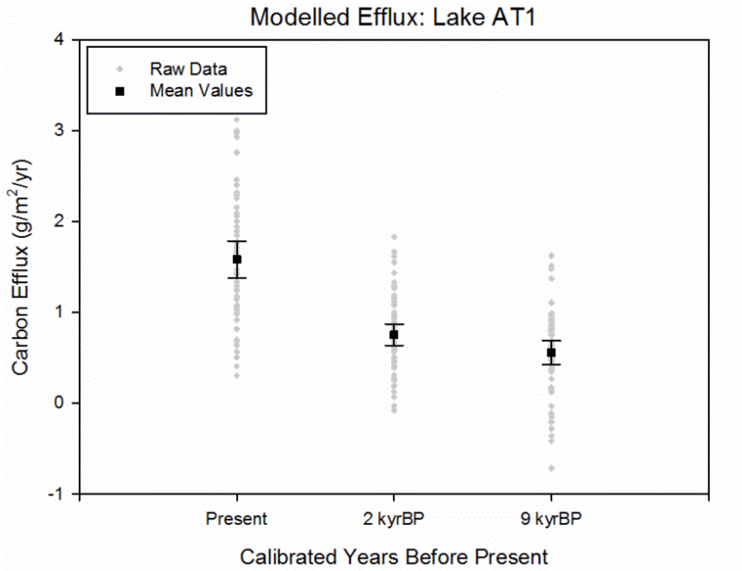

Figure 28. Modelling results from the coupled version of PALM showing the rate of CO_2 efflux in AT1 for the time slices of interest.

Table 18. Ratios of allochthonous or autochthonous in Lake AT1 during the time slices of interest.

Time	Present	2 kyrBP	9 kyrBP
AL:AU	0.0668	0.0598	0.0587

Discussion

4.1 Implications of Results

The realistic integration of lake and catchment carbon dynamics has only occurred in the past few years. Thus, the first outcome of this project is the knowledge that modelling paleo lake carbon cycling is indeed possible given the present lake, terrestrial, and climate models. PALM was able to model reasonable carbon fluxes across a wide range of values observed in the Arctic, as well as, two different coupled lake-catchment systems when forced with paleoclimatic data. LPJ-GUESS was not able to model PFT percent cover for Ruppert Lake that corresponded well with either the satellite based classification or the predicted PFT percent covers which were based on the paleo pollen data. Some of this may be attributed to uncertainties in the input data, however, it also partially appears to be a systemic problem linked to the way LPJ-GUESS limits vegetation growth. Nevertheless, forcing LPJ-GUESS to model a moderately reasonable approximation of the catchment is relatively straightforward. Moreover, the vegetation was responsive to change within climatic conditions within a given time period. LPJ-GUESS was linked to PALM and with some modification and a suitable data set for calibration a potential exists to link the two models without utilizing a look-up table. While time constraints prevented PALM from being fleshed out and the approximations for terrestrial input would benefit from some adjustments, this works gives proof of concept and a solid base that can be expanded upon.

The preliminary results analysed in this document corroborate the assertions of many lake and climate scientist that Arctic warming will lead to more carbon sequestration in lakes (Adrian *et al.*, 2009, Benoy *et al.*, 2007, Cardille *et al.*, 2009). However, results from Lake AT1 and the sensitivity analysis also indicate that with increases in catchment carbon and increased temperature, lake carbon efflux can also be expected to rise. The modelled effluxes from Ruppert Lake, further complicates matters as it shows much greater intre-annual variation than variation between the time slices of interest. Furthermore, because uncertainties surround the magnitude of modelled sedimentation and efflux, no conclusions on the climate forcing potential of lakes in the future or past can currently be drawn.

4.2 Effects of Modelling Assumptions

4.2.1 LPJ-GUESS

4.2.1.1 Topography

LPJ-GUESS models an area by simulating a flat surface. Although LPJ-GUESS does show different PFTs in mountainous areas this is due to lower surface temperatures occurring at higher elevations. Slope and aspect of an area are key determining factors in plant distribution and they affect illumination, hydrology, and soil perturbation. The exclusion of slope and aspect from LPJ-GUESS create a fundamental flaw in the model when trying to predict vegetation cover on the catchment scale. Recent work done by Tang *et al.* (2013) has begun to rectify this problem. In their work Tang *et al.* (2013) greatly improve the modelled quantity and timing of runoff events in three Swedish catchments increasing the R^2 value from 0.4 to 0.8 by modifying LPJ-GUESS to incorporate topography. This updated version of LPJ-GEUSS was not applied in this study because it was developed only recently and it presents a tendency to overestimate the amount of incoming runoff. The difference in runoff between the older version of LPJ-GUESS used in this study and the observed data was between 0 and 20 mm per month or at most around 2 mm per day. Thus, the old version was deemed more suited for this exercise, however, the underestimation of runoff caused by this is a likely contributor to the very low observed sedimentation rates and low AL:AU ratio for carbon entering the sediment. Nevertheless, even with the improvements in modelling hydrology the Tang *et al.* version of simulating topography still falls short of the ideal as it is not used to update LPJ-GUESS' bioclimatic limits.

4.2.1.2 Bioclimatic Limits

The way LPJ-GUESS limits vegetation growth is thought to be one of the main sources of error with regards to the unrealistic percent PFT covers modelled for the paleo periods in this study. At Ruppert Lake the CLM cover type is severely underestimated. This is likely because the presence of this cover type is caused by changes in topography and resulting exposure to harsh conditions. The current iteration of LPJ-GUESS is unable to take such conditions into account. One of the assumptions made during the course of this project was that the bioclimatic limit *zero_max* should be removed from the PDS, CLM, and GFT plant functional types. This was done because these PFTs were known to occur in our study areas and were exhibiting a LAI of 0 even with all other PFTs switched off. Effectively, even without any competition for resources these PFTs would not grow with the given input. A growing degree day is defined as day in which the average daily temperature is above a threshold value, in the case of LPJ-GUESS 0° C, above which plant growth can occur. The variable, *zero_max*, which was altered during the course of this work, caps the maximum amount of growing degrees for a PFT. In terms of plant physiology, a cap on the number of growing degree days does not make sense. Why would growth be limited by a high number of days exhibiting suitable growing conditions? One could argue that *zero_max* functions in order to account for drought stress or temperature stress, however, both of these bioclimatic limits are already included in the model as separate limits. The bioclimatic limit *zero_max* is, in fact, not applied to any of the other PFTs. Wolf *et al.* (2008), who added this limit to the model, state that is was done specifically to limit the prevalence of these PFTs because were outcompeting grass in a manner that did not represent what was observed in their study area. This is an example of LPJ-GUESS being tailored to show the expected PFTs not by actual plant physiology or completion but by the desire to represent PFTs in the distribution they are observed in. With the limit removed the PFTs did not become overly abundant showing that their growth was sufficiently limited by the other bioclimatic limits.

4.2.1.3 PALM

The current iteration of PALM contains numerous assumptions that may be introducing error into the model's output. The models on which PALM was based also contained their own sets of assumptions that could act as sources of error. In Cardille et al.'s 2007 study, three of the lakes were monitored intensively for validation. The amount of inorganic carbon within the lakes was modelled to a high degree of accuracy but there was a bit more discrepancy where organic carbon was concerned. Though the model was able to accurately gage the mean annual amount of dissolved organic carbon (DOC), the monthly totals of DOC varied in almost an inverse pattern to the observed values. This is concerning as it may indicate that the model does not have the correct underlying principles. Furthermore, variables, like the rates of decomposition, taken from Hanson *et al.* (2004) may not be universally applicable and could be causing systematic errors. The modifications made to PALM may also cause some issues. The modelling of the lakes as seepage lakes is a major assumption whose validity cannot realistically be tested. Retention time of carbon in lakes is one of the major factors controlling its cycling. The assumption that no outflows to the lakes exist is a major assumption that undermines the validity of the PALM model. Furthermore, PALM does not currently model water flows. While this assumption simplifies the model its effect on the accuracy of the modelled carbon cycling is unknown, and may be very significant as lake volume and surface are have been shown to significantly impact the modelled carbon dynamics. Also, PALM only currently models one biotic component of the lake system. There is evidence that Ruppert Lake has had aquatic vegetation since around 10 kyrBP (Van Hardenbroek, 2014) and there is speculation that this lake is dominated by benthic production (Anderson, 2014). Any further work done with PALM will need to address these issues.

4.3 Possible Sources of Sedimentation Underestimation

The low rate of sediment accumulation is in all probability due to the underestimation of allochthonous carbon input. However, whether it is the POC loading from aerial deposition or the POC derived from catchment runoff that is being underestimated remains unclear. The concentration of POC in runoff coming from the catchment was set to a very high concentration, around 1 g m^{-3}, considering the average POC concentration for stream water in the Kling (2013). Within the LTER dataset the mean concentration was 0.307 g m^{-3}. While the concentration of POC in the runoff may be high the volume of runoff used for this experiment is known to be underestimated. Additionally, as mentioned previously, the catchment areas used for this study were also underestimated. A contour map of the Ruppert Lake was digitized to produce the lake’s catchment area for comparison. Standard methods of drainage basin delineation produced a catchment of ~ 400 ha. This size for the catchment was clearly an overestimate, as it included a number of other lake catchments, and likely due to the scale of the map. However, a realistic estimate of the true drainage basin of Ruppert lake probably falls between the value used for this study, ~ 40 ha, and the 400 ha estimated from the topographic map. When one combines the underestimation of runoff due to catchment area and that due to LPJ-GUESS’ underestimation of runoff, it seems very likely that the volume of runoff is the main source of error in the underestimation of sedimentation.

4.4 Proposed Improvements

4.4.1 Additional Modules for PALM

Many features, such as modelling light absorption by organic matter or methane production, could be added to PALM. But prior to these additions, two process have been identified that would greatly improve the stock that can be placed in PALMs modelled output.

Dynamic process based models for simulating lake temperature are common and have been shown to function to a high degree of accuracy (Gudasz *et al.*, 2010, Piccolroaz *et al.*, 2013, Gal *et al.*, 2009, Wu *et al.*, 2013). As lake temperature is such an important factor in determining carbon dynamics for PALM, evidenced by the sensitivity analysis (Table 10), it is imperative that any future work done with PALM should incorporate such a module. The input data required to run these modules are already available, even for the paleo time slices. The only inputs required are surface air temperature and incoming solar radiation (Piccolroaz *et al.*, 2013).

Another necessary modification to PALM is the modelling of water fluxes. Although fixing the lake volume during the PALM runs did eliminate a variable and made identifying the model's driving forces simpler, as the sensitivity analysis showed (Table 10) lake volume and surface area play a significant role in the modelled outputs. It would be interesting to see how a dynamic model capable of modelling monthly variation of these factors would affect the results. Modelling water dynamics is standard fare in lake modelling and equations from other models, such as the one described in Wu *et al.* (2013), could be incorporated in a subsequent version of PALM.

4.4.2 Directly Modelling DOC and POC from LPJ-GUESS

LPJ-GUESS has three carbon pools that represent soil carbon. The first pool, denoted as 'litter', is created by leaf/needle fall and the plant mortality. It is from this pool that POC was assumed to stem from. The other two pools, denoted as 'soil fast' and 'soil slow' are the sources of DOC. 'Soil fast' indicates carbon that has a faster decay rate, such as dead fine root matter. Soil temperature and water content are cited as being the major environmental factors affecting decomposition and the production of DOC within soils (Zhang *et al.*, 2013a, Wu *et al.*, 2013). The rate of heterotrophic respiration, which is given as a monthly output, takes both soil moisture and temperature into account. Thus, it was assumed that heterotrophic respiration could be linked to the amount of available DOC for transport. If this is accomplished successfully, PALM could be applied in any environment, given that LPJ-GEUSS can be applied for any region of the globe.

4.4.3 Incorporation of Remote Sensing

For this study most of the lakes' water quality characteristics were derived from samples collected in the field. For remote areas such as the Arctic this is non-ideal, as a vast number of lakes exist in the region and the majority of them are inaccessible. Remote sensing of the lakes' water quality and physical characteristics would enable PALM's application in remote regions and on a large spatial scale. Deriving bathymetric measurements via remote sensing is well established and can be done to the same, if not a higher, degree of accuracy than ground based methods of measurement (Legleiter and Roberts, 2009, Hamilton *et al.*, 1993, Mueller, Crétaux and Birkett, 2006). Moreover, remote sensing has been used to model particulate matter in the form of lake turbidity to a high degree of accuracy (Binding *et al.*, 2008, McCullough *et al.*, 2012). Remote sensing has even been used to map submerged aquatic vegetation (Wolter *et al.*, 2005, Heblinski *et al.*, 2011). One issue that remote senescing has a bit more difficulty with is DOC. Techniques have been derived to accurately model DOC, however, their accuracy is limited by the spatial resolution of the available satellite data and the existing models tend to be specific for particular lakes or regions (Kutser, 2012, Jacobsson, 2014, Brezonik *et al.*, 2005). This is in large part due to the fact that not all DOC is coloured and the ratio of coloured to transparent DOC varies between catchments . Moreover, this ratio may also vary temporally within a catchment. For example, Olefeldt *et al.* (2013) found that the proportion of pigmented DOC dropped after the catchment experienced a fire. They ascribed this to increase exposure of the soil to UV-light, as pigmented molecules are very absorptive and tend to be degraded with prolonged exposure. Despite this possible complication, the integration of PALM with remotely sensed data remains promising.

Conclusions

The novel approach taken by this study, despite its limitations, shows a strong potential for the modelling of carbon cycling in Arctic lakes. The coupling of LPJ-GUESS with PALM was able to shed some light on the observed changes in carbon sedimentation rate within Ruppert Lake and Lake AT1. Despite the many possible sources of error, when forced with the paleo-climatic data, the integrated models simulated a very similar pattern of sedimentation to what is observed in Ruppert Core B. While the pattern in sedimentation observed in AT1 did not fit with the lake core data, it did indicate that the change in PFTs had a very pronounced effect on the lake's carbon cycling. The results from AT1 also indicate that a lake's trophic state is not fixed during the course of its ontogeny.

Significant improvements to PALM and its integration with catchment carbon export must be made before any quantitative results from this model can be drawn. There is a great necessity for further model validation and calibration on observed lake systems. However, many improvements could be made with relative ease. These additions were beyond the scope of this research and were not incorporated in this study in order to avoid a model with too many interrelated driving components.

The results of this project will potentially aid the LAC project in the interpretation of paleolimnological data obtained from their study cites.

References

Achberger, C., Ackerman, S. A., Ahlstrom, A., Alfaro, E. J., Allan, R. J., Alves, L., Amador, J. A., Amelie, V., Andrianjafinirina, S., Antonov, J., Arndt, D. S., Ashik, I., Atheru, Z., Attaher, S. M., Baez, J., Banzon, V., Baringer, M. O., Barreira, S., Barriopedro, D., Barthia, P. K., Beal, L. M., Becker, A., Behrenfeld, M. J., Bell, G. D., Belward, A. S., Benedetti, A., Berrisford, P., Berry, D. I., Beszczynska-Moeller, A., Bhatt, U. S., Bidegain, M., Bindoff, N. L., Bissolli, P., Blake, E. S., Blunden, J., Booneeady, P., Bosilovich, M. G., Boudet, D. R., Box, J. E., Boyer, T. P., Bromwich, D. H., Brown, R., Bryden, H. L., Bulygina, O. N., Burrows, J., Butler, J., Cais, P., Calderon, B., Callaghan, T. V., Camargo, S. J., Cappelen, J., Carmack, E., Chambers, D. P., Chelliah, M., Chidichimo, M. P., Christiansen, H., Christy, J., Coelho, C. a. S., Colwell, S., Comiso, J. C., Compo, G. P., Crouch, J., Cunningham, S. A., Cutie, V. C., Dai, A. G., Davydova-Belitskaya, V., De Jeu, R., Decker, D., Dee, D., Demircan, M., Derksen, C., Diamond, H. J., Dlugokencky, E. J., Dohan, K., Dolman, A. J., Dorigo, W., Drozdov, D. S., Durack, P. J., Dutton, G. S., Easterling, D., Ebita, A., Eischeid, J., Elkins, J. W., Epstein, H. E., Euscategui, C., Faijka-Williams, E., Famiglietti, J. S., Faniriantsoa, R., Feely, R. A., Fekete, B. M., Fenimore, C., Fettweis, X., Fields, E., Fioletov, V. E., Fogarty, V. E., Fogt, R. L., Forbes, B. C., Foster, M. J., Frajka-Williams, E., Free, M., et al. 2011. STATE OF THE CLIMATE IN 2010. *Bulletin of the American Meteorological Society,* 92**,** S17-+.

Adrian, R., O'reilly, C. M., Zagarese, H., Baines, S. B., Hessen, D. O., Keller, W., Livingstone, D. M., Sommaruga, R., Straile, D., Van Donk, E., Weyhenmeyer, G. A. & Winder, M. 2009. Lakes as sentinels of climate change. *Limnology and Oceanography,* 54**,** 2283-2297.

Ahlstrom, A., Schurgers, G., Arneth, A. & Smith, B. 2012. Robustness and uncertainty in terrestrial ecosystem carbon response to CMIP5 climate change projections. *Environmental Research Letters,* 7**,** 9.

Aitkenhead-Peterson, J., Mcdowell, W., Neff, J., Stuart, E. & Robert, L. 2003. *Sources, production, and regulation of allochthonous dissolved organic matter inputs to surface waters*, Academic Press San Diego.

Algesten, G., Sobek, S., Bergstrom, A. K., Agren, A., Tranvik, L. J. & Jansson, M. 2004. Role of lakes for organic carbon cycling in the boreal zone. *Global Change Biology,* 10**,** 141-147.

Allen, J. R. M., Hickler, T., Singarayer, J. S., Sykes, M. T., Valdes, P. J. & Huntley, B. 2010. Last glacial vegetation of northern Eurasia. *Quaternary Science Reviews,* 29**,** 2604-2618.

Anderson, L. G. 2014.

Anderson, N. J., Liversidge, A. C., Mcgowan, S. & Jones, M. D. 2012. Lake and catchment response to Holocene environmental change: spatial variability along a climate gradient in southwest Greenland. *Journal of Paleolimnology,* 48**,** 209-222.

Baird, C. & Cann, M. 2005. *Environmental chemistry*, Macmillan.

Benoy, G., Cash, K., Mccauley, E. & Wrona, F. 2007. Carbon dynamics in lakes of the boreal forest under a changing climate. *Environmental Reviews,* 15**,** 175-189.

Biddanda, B. & Benner, R. 1997. Carbon, nitrogen, and carbohydrate fluxes during the production of particulate and dissolved organic matter by marine phytoplankton. *Limnology and Oceanography,* 42**,** 506-518.

Binding, C. E., Jerome, J. H., Bukata, R. P. & Booty, W. G. 2008. Spectral absorption properties of dissolved and particulate matter in Lake Erie. *Remote Sensing of Environment,* 112**,** 1702-1711.

Binney, H. A., Gething, P. W., Nield, J. M., Sugita, S. & Edwards, M. E. 2011. Tree line identification from pollen data: beyond the limit? *Journal of Biogeography,* 38**,** 1792-1806.

Brett, M. T., Arhonditsis, G. B., Chandra, S. & Kainz, M. J. 2012. Mass Flux Calculations Show Strong Allochthonous Support of Freshwater Zooplankton Production Is Unlikely. *Plos One,* 7.

Brezonik, P., Menken, K. D. & Bauer, M. 2005. Landsat-based remote sensing of lake water quality characteristics, including chlorophyll and colored dissolved organic matter (CDOM). *Lake and Reservoir Management,* 21**,** 373-382.

Brubaker, L. B., Higuera, P. E., Rupp, T. S., Olson, M. A., Anderson, P. M. & Hu, F. S. 2009. Linking sediment-charcoal records and ecological modeling to understand causes of fire-regime change in boreal forests. *Ecology,* 90**,** 1788-1801.

Buffam, I., Turner, M. G., Desai, A. R., Hanson, P. C., Rusak, J. A., Lottig, N. R., Stanley, E. H. & Carpenter, S. R. 2011. Integrating aquatic and terrestrial components to construct a complete carbon budget for a north temperate lake district. *Global Change Biology,* 17**,** 1193-1211.

Cardille, J. A., Carpenter, S. R., Coe, M. T., Foley, J. A., Hanson, P. C., Turner, M. G. & Vano, J. A. 2007. Carbon and water cycling in lake-rich landscapes: Landscape connections, lake hydrology, and biogeochemistry. *Journal of Geophysical Research-Biogeosciences,* 112.

Cardille, J. A., Carpenter, S. R., Foley, J. A., Hanson, P. C., Turner, M. G. & Vano, J. A. 2009. Climate change and lakes: Estimating sensitivities of water and carbon budgets. *Journal of Geophysical Research-Biogeosciences,* 114.

Christensen, T. R., Johansson, T., Olsrud, M., Ström, L., Lindroth, A., Mastepanov, M., Malmer, N., Friborg, T., Crill, P. & Callaghan, T. V. 2007. A catchment-scale carbon and greenhouse gas budget of a subarctic landscape. *Philosophical Transactions of the Royal Society A: Mathematical, Physical and Engineering Sciences,* 365**,** 1643-1656.

Cole, J. J., Bade, D. L., Bastviken, D., Pace, M. L. & Van De Bogert, M. 2010. Multiple approaches to estimating air-water gas exchange in small lakes. *Limnology and Oceanography-Methods,* 8**,** 285-293.

Cole, J. J., Carpenter, S. R., Kitchell, J. F. & Pace, M. L. 2002. Pathways of organic carbon utilization in small lakes: Results from a whole-lake C-13 addition and coupled model. *Limnology and Oceanography,* 47**,** 1664-1675.

Cole, J. J., Prairie, Y. T., Caraco, N. F., Mcdowell, W. H., Tranvik, L. J., Striegl, R. G., Duarte, C. M., Kortelainen, P., Downing, J. A., Middelburg, J. J. & Melack, J. 2007. Plumbing the global carbon cycle: Integrating inland waters into the terrestrial carbon budget. *Ecosystems,* 10**,** 171-184.

Cole, T. M. & Buchak, E. M. 1995. CE-QUAL-W2: A Two-Dimensional, Laterally Averaged, Hydrodynamic and Water Quality Model, Version 2.0. User Manual. DTIC Document.

Connolly, J. P. & Coffin, R. B. 1995. MODEL OF CARBON CYCLING IN PLANKTONIC FOOD WEBS. *Journal of Environmental Engineering-Asce,* 121**,** 682-690.

Crétaux, J.-F. & Birkett, C. 2006. Lake studies from satellite radar altimetry. *Comptes Rendus Geoscience,* 338**,** 1098-1112.

Daly, C., Bachelet, D., Lenihan, J. M., Neilson, R. P., Parton, W. & Ojima, D. 2000. Dynamic simulation of tree-grass interactions for global change studies. *Ecological Applications,* 10**,** 449-469.

Debele, B., Srinivasan, R. & Parlange, J.-Y. 2008. Coupling upland watershed and downstream waterbody hydrodynamic and water quality models (SWAT and CE-QUAL-W2) for better water resources management in complex river basins. *Environmental modeling & assessment,* 13**,** 135-153.

Deng, B., Liu, S. D., Xiao, W., Wang, W., Jin, J. M. & Lee, X. H. 2013. Evaluation of the CLM4 Lake Model at a Large and Shallow Freshwater Lake. *Journal of Hydrometeorology,* 14**,** 636-649.

Dickens, A. F., Baldock, J., Kenna, T. C. & Eglinton, T. I. 2011. A depositional history of particulate organic carbon in a

floodplain lake from the lower Ob'River, Siberia. *Geochimica et Cosmochimica Acta,* 75**,** 4796-4815.
Dillon, P. J. & Molot, L. A. 1997. Dissolved organic and inorganic carbon mass balances in central Ontario lakes. *Biogeochemistry,* 36**,** 29-42.
Domis, L. N. D. S., Elser, J. J., Gsell, A. S., Huszar, V. L. M., Ibelings, B. W., Jeppesen, E., Kosten, S., Mooij, W. M., Roland, F., Sommer, U., Van Donk, E., Winder, M. & Lurling, M. 2013. Plankton dynamics under different climatic conditions in space and time. *Freshwater Biology,* 58**,** 463-482.
Downing, J. A., Prairie, Y. T., Cole, J. J., Duarte, C. M., Tranvik, L. J., Striegl, R. G., Mcdowell, W. H., Kortelainen, P., Caraco, N. F., Melack, J. M. & Middelburg, J. J. 2006. The global abundance and size distribution of lakes, ponds, and impoundments. *Limnology and Oceanography,* 51**,** 2388-2397.
Edwards, J. M. 2013.
Edwards, M. E., Mock, C. J., Finney, B. P., Barber, V. A. & Bartlein, P. J. 2001. Potential analogues for paleoclimatic variations in eastern interior Alaska during the past 14,000 yr: atmospheric-circulation controls of regional temperature and moisture responses. *Quaternary Science Reviews,* 20**,** 189-202.
Eisenreich, S. J., Looney, B. B. & Thornton, J. D. 1981. Airborne organic contaminants in the Great Lakes ecosystem. *Environmental Science & Technology,* 15**,** 30-38.
Epstein, H. E., Myers-Smith, I. & Walker, D. A. 2013. Recent dynamics of arctic and sub-arctic vegetation. *Environmental Research Letters,* 8.
Fee, E. J., Hecky, R. E., Kasian, S. E. M. & Cruikshank, D. R. 1996. Effects of lake size, water clarity, and climatic variability on mixing depths in Canadian Shield lakes. *Limnology and Oceanography,* 41**,** 912-920.
Foley, J. A., Prentice, I. C., Ramankutty, N., Levis, S., Pollard, D., Sitch, S. & Haxeltine, A. 1996. An integrated biosphere model of land surface processes, terrestrial carbon balance, and vegetation dynamics. *Global Biogeochemical Cycles,* 10**,** 603-628.
Fortino, K., Whalen, S. C. & Johnson, C. R. 2014. Relationships between lake transparency, thermocline depth, and sediment oxygen demand in Arctic lakes. *Inland Waters,* 4**,** 79-90.
Futter, M. N., Butterfield, D., Cosby, B. J., Dillon, P. J., Wade, A. J. & Whitehead, P. G. 2007. Modeling the mechanisms that control in-stream dissolved organic carbon dynamics in upland and forested catchments. *Water Resources Research,* 43**,** 16.

Gal, G., Hipsey, M. R., Parparov, A., Wagner, U., Makler, V. & Zohary, T. 2009. Implementation of ecological modeling as an effective management and investigation tool: Lake Kinneret as a case study. *Ecological Modelling,* 220**,** 1697-1718.

Garreta, V., Guiot, J., Mortier, F., Chadoeuf, J. & Hely, C. 2012. Pollen-based climate reconstruction: Calibration of the vegetation-pollen processes. *Ecological Modelling,* 235**,** 81-94.

Grimm, N. B., Gergel, S. E., Mcdowell, W. H., Boyer, E. W., Dent, C. L., Groffman, P., Hart, S. C., Harvey, J., Johnston, C., Mayorga, E., Mcclain, M. E. & Pinay, G. 2003. Merging aquatic and terrestrial perspectives of nutrient biogeochemistry. *Oecologia,* 137**,** 485-501.

Gudasz, C., Bastviken, D., Steger, K., Premke, K., Sobek, S. & Tranvik, L. J. 2010. Temperature-controlled organic carbon mineralization in lake sediments. *Nature,* 466**,** 478-U3.

Guth, P. Geomorphometric comparison of ASTER GDEM and SRTM. A special joint symposium of ISPRS Technical Commission IV & AutoCarto in conjunction with ASPRS/CaGIS, 2010.

Hamilton, M. K., Davis, C. O., Rhea, W. J., Pilorz, S. H. & Carder, K. L. 1993. Estimating chlorophyll content and bathymetry of Lake Tahoe using AVIRIS data. *Remote Sensing of Environment,* 44**,** 217-230.

Hanson, P. C., Bade, D. L., Carpenter, S. R. & Kratz, T. K. 2003. Lake metabolism: Relationships with dissolved organic carbon and phosphorus. *Limnology and Oceanography,* 48**,** 1112-1119.

Hanson, P. C., Hamilton, D. P., Stanley, E. H., Preston, N., Langman, O. C. & Kara, E. L. 2011. Fate of Allochthonous Dissolved Organic Carbon in Lakes: A Quantitative Approach. *Plos One,* 6.

Hanson, P. C., Pollard, A. I., Bade, D. L., Predick, K., Carpenter, S. R. & Foley, J. A. 2004. A model of carbon evasion and sedimentation in temperate lakes. *Global Change Biology,* 10**,** 1285-1298.

Haxeltine, A. & Prentice, I. C. 1996. BIOME3: An equilibrium terrestrial biosphere model based on ecophysiological constraints, resource availability, and competition among plant functional types. *Global Biogeochemical Cycles,* 10**,** 693-709.

Heblinski, J., Schmieder, K., Heege, T., Agyemang, T. K., Sayadyan, H. & Vardanyan, L. 2011. High-resolution satellite remote sensing of littoral vegetation of Lake Sevan (Armenia) as a basis for monitoring and assessment. *Hydrobiologia,* 661**,** 97-111.

Hessen, D. O., Blomqvist, P., Dahl-Hansen, G., Drakare, S. & Lindstrom, E. S. 2004. Production and food web interactions of

Arctic freshwater plankton and responses to increased DOC. *Archiv Fur Hydrobiologie,* 159**,** 289-307.

Higuera, P. E., Brubaker, L. B., Anderson, P. M., Hu, F. S. & Brown, T. A. 2009. Vegetation mediated the impacts of postglacial climate change on fire regimes in the south-central Brooks Range, Alaska. *Ecological Monographs,* 79**,** 201-219.

Higuera, P. E., Chipman, M. L., Barnes, J. L., Urban, M. A. & Hu, F. S. 2011. Variability of tundra fire regimes in Arctic Alaska: millennial-scale patterns and ecological implications. *Ecological Applications,* 21**,** 3211-3226.

Houser, J. N. 2001. *Dissolved organic carbon in lakes: Effects on thermal structure, primary production, and hypolimnetic metabolism*, University of Wisconsin--Madison.

Huntley, B., Allen, J. R. M., Collingham, Y. C., Hickler, T., Lister, A. M., Singarayer, J., Stuart, A. J., Sykes, M. T. & Valdes, P. J. 2013. Millennial Climatic Fluctuations Are Key to the Structure of Last Glacial Ecosystems. *PLoS ONE,* 8**,** e61963.

Jacobsson, J. 2014. The Suitability of Using Landsat TM-5 Images for Estimating Chromophoric Dissolved Organic Matter in Subarctic Lakes.

Jansson, M., Bergstrom, A. K., Blomqvist, P. & Drakare, S. 2000. Allochthonous organic carbon and phytoplankton/bacterioplankton production relationships in lakes. *Ecology,* 81**,** 3250-3255.

Jarvis, S. 2012. *Optimising, Understanding and Quantifying Itrax XRF Data.* Doctor of Philosophy, UNIVERSITY OF SOUTHAMPTON.

Jones, B. 2013. *Circumarctic Lakes Observation Network* [Online]. USGS. Available: http://www.usgs.gov/climate_landuse/lcs/projects/calon.asp [Accessed 5-18-2014.

Jonsson, A., Algesten, G., Bergstrom, A. K., Bishop, K., Sobek, S., Tranvik, L. J. & Jansson, M. 2007. Integrating aquatic carbon fluxes in a boreal catchment carbon budget. *Journal of Hydrology,* 334**,** 141-150.

Kittel, T. G. F., Steffen, W. L. & Chapin, F. S. 2000. Global and regional modelling of Arctic-boreal vegetation distribution and its sensitivity to altered forcing. *Global Change Biology,* 6**,** 1-18.

Klimaszyk, P. & Rzymski, P. 2013. Catchment vegetation can trigger lake dystrophy through changes in runoff water quality. *Annales De Limnologie-International Journal of Limnology,* 49**,** 191-197.

Kling, G., Kipphut, G. & Miller, M. 1992. The flux of CO2 and CH4 from lakes and rivers in arctic Alaska. *Hydrobiologia,* 240**,** 23-36.

Kling, G. W. 2013. *Biogeochemistry data set for soil waters, streams, and lakes near Toolik on the North Slope of Alaska.,* knb-lter-arc.10279.1

Kortelainen, P., Rantakari, M., Huttunen, J. T., Mattsson, T., Alm, J., Juutinen, S., Larmola, T., Silvola, J. & Martikainen, P. J. 2006. Sediment respiration and lake trophic state are important predictors of large CO2 evasion from small boreal lakes. *Global Change Biology,* 12**,** 1554-1567.

Kortelainen, P., Rantakari, M., Pajunen, H., Huttunen, J. T., Mattsson, T., Juutinen, S., Larmola, T., Alm, J., Silvola, J. & Martikainen, P. J. 2013. Carbon evasion/accumulation ratio in boreal lakes is linked to nitrogen. *Global Biogeochemical Cycles,* 27**,** 363-374.

Kutser, T. 2012. The possibility of using the Landsat image archive for monitoring long time trends in coloured dissolved organic matter concentration in lake waters. *Remote Sensing of Environment,* 123**,** 334-338.

Legleiter, C. J. & Roberts, D. A. 2009. A forward image model for passive optical remote sensing of river bathymetry. *Remote Sensing of Environment,* 113**,** 1025-1045.

Liversidge, A. C. 2012. *The role of climate in determining the ontogeny trends of low Arctic lakes, south-western Greenland.* © Antonia Claire Liversidge.

Los, H. 2009. *Eco-hydrodynamic modelling of primary production in coastal waters and lakes using BLOOM*, Ios Press.

Lottig, N. R., Stanley, E. H., Hanson, P. C. & Kratz, T. K. 2011. Comparison of regional stream and lake chemistry: Differences, similarities, and potential drivers. *Limnology and Oceanography,* 56**,** 1551-1562.

Luoto, T. P. & Ojala, A. E. K. 2014. Paleolimnological assessment of ecological integrity and eutrophication history for Lake Tiilaanjarvi (Askola, Finland). *Journal of Paleolimnology,* 51**,** 455-468.

Lurling, M. & Domis, L. N. D. S. 2013. Predictability of plankton communities in an unpredictable world. *Freshwater Biology,* 58**,** 455-462.

Mackay, M. D., Neale, P. J., Arp, C. D., Domis, L. N. D., Fang, X., Gal, G., Johnk, K. D., Kirillin, G., Lenters, J. D., Litchman, E., Macintyre, S., Marsh, P., Melack, J., Mooij, W. M., Peeters, F., Quesada, A., Schladow, S. G., Schmid, M., Spence, C. & Stokesr, S. L. 2009. Modeling lakes and reservoirs in the climate system. *Limnology and Oceanography,* 54**,** 2315-2329.

MacIntyre, S. 2000. Water temperatures from Toolik Lake in Summer 1998. *knb-lter-arc.10406.1.*

Makler-Pick, V., Gal, G., Gorfine, M., Hipsey, M. R. & Carmel, Y. 2011. Sensitivity analysis for complex ecological models - A new approach. *Environmental Modelling & Software,* 26**,** 124-134.
Mccullough, I. M., Loftin, C. S. & Sader, S. A. 2012. Combining lake and watershed characteristics with Landsat TM data for remote estimation of regional lake clarity. *Remote Sensing of Environment,* 123**,** 109-115.
Mcdowell, W. H. 2003. Dissolved organic matter in soils—future directions and unanswered questions. *Geoderma,* 113**,** 179-186.
Mcguire, A. D., Anderson, L. G., Christensen, T. R., Dallimore, S., Guo, L. D., Hayes, D. J., Heimann, M., Lorenson, T. D., Macdonald, R. W. & Roulet, N. 2009. Sensitivity of the carbon cycle in the Arctic to climate change. *Ecological Monographs,* 79**,** 523-555.
Mcmanus, K. M., Morton, D. C., Masek, J. G., Wang, D., Sexton, J. O., Nagol, J. R., Ropars, P. & Boudreau, S. 2012. Satellite-based evidence for shrub and graminoid tundra expansion in northern Quebec from 1986 to 2010. *Global Change Biology,* 18**,** 2313-2323.
Melillo, J. M., Borchers, J., Chaney, J., Fisher, H., Fox, S., Haxeltine, A., Janetos, A., Kicklighter, D. W., Kittel, T. G. F., Mcguire, A. D., Mckeown, R., Neilson, R., Nemani, R., Ojima, D. S., Painter, T., Pan, Y., Parton, W. J., Pierce, L., Pitelka, L., Prentice, C., Rizzo, B., Rosenbloom, N. A., Running, S., Schimel, D. S., Sitch, S., Smith, T. & Woodward, I. 1995. VEGETATION ECOSYSTEM MODELING AND ANALYSIS PROJECT - COMPARING BIOGEOGRAPHY AND BIOGEOCHEMISTRY MODELS IN A CONTINENTAL-SCALE STUDY OF TERRESTRIAL ECOSYSTEM RESPONSES TO CLIMATE-CHANGE AND CO2 DOUBLING. *Global Biogeochemical Cycles,* 9**,** 407-437.
Miller, P. A., Giesecke, T., Hickler, T., Bradshaw, R. H. W., Smith, B., Seppa, H., Valdes, P. J. & Sykes, M. T. 2008. Exploring climatic and biotic controls on Holocene vegetation change in Fennoscandia. *Journal of Ecology,* 96**,** 247-259.
Miller, P. A. & Smith, B. 2012. Modelling Tundra Vegetation Response to Recent Arctic Warming. *Ambio,* 41**,** 281-291.
Mooij, W. M., Trolle, D., Jeppesen, E., Arhonditsis, G., Belolipetsky, P. V., Chitamwebwa, D. B. R., Degermendzhy, A. G., Deangelis, D. L., Domis, L. N. D., Downing, A. S., Elliott, J. A., Fragoso, C. R., Gaedke, U., Genova, S. N., Gulati, R. D., Hakanson, L., Hamilton, D. P., Hipsey, M. R., T Hoen, J., Hulsmann, S., Los, F. H., Makler-Pick, V., Petzoldt, T., Prokopkin, I. G., Rinke, K., Schep, S. A., Tominaga, K., Van Dam, A. A., Van Nes, E. H.,

Wells, S. A. & Janse, J. H. 2010. Challenges and opportunities for integrating lake ecosystem modelling approaches. *Aquatic Ecology,* 44**,** 633-667.

Mueller, R. Utilizing Geographic Information Science Advancements For Bathymetric Mapping and Dredging Assessment of a Small Urban Lake in Southeastern Minnesota.

Neff, J. C. & Asner, G. P. 2001. Dissolved Organic Carbon in Terrestrial Ecosystems: Synthesis and a Model. *Ecosystems,* 4**,** 29-48.

Neilson, R. P. 1995. A MODEL FOR PREDICTING CONTINENTAL-SCALE VEGETATION DISTRIBUTION AND WATER-BALANCE. *Ecological Applications,* 5**,** 362-385.

Olefeldt, D., Turetsky, M. R. & Blodau, C. 2013. Altered Composition and Microbial versus UV-Mediated Degradation of Dissolved Organic Matter in Boreal Soils Following Wildfire. *Ecosystems,* 16**,** 1396-1412.

Pacheco, F. S., Roland, F. & Downing, J. A. 2013. Eutrophication reverses whole-lake carbon budgets. *Inland Waters,* 4**,** 41-48.

Paltan Lopez, H. 2013. *Methane fluxes from Arctic lakes.* MSc, University of Southampton.

Parparov, A. & Gal, G. 2012. Assessment and implementation of a methodological framework for sustainable management: Lake Kinneret as a case study. *Journal of Environmental Management,* 101**,** 111-117.

Pearson, R. G., Phillips, S. J., Loranty, M. M., Beck, P. S. A., Damoulas, T., Knight, S. J. & Goetz, S. J. 2013. Shifts in Arctic vegetation and associated feedbacks under climate change. *Nature Climate Change,* 3**,** 673-677.

Perroud, M. & Goyette, S. 2012. Interfacing a one-dimensional lake model with a single-column atmospheric model: 2. Thermal response of the deep Lake Geneva, Switzerland under a 2 x CO2 global climate change. *Water Resources Research,* 48.

Pfeiffer, M., Spessa, A. & Kaplan, J. O. 2013. A model for global biomass burning in preindustrial time: LPJ-LMfire (v1.0). *Geoscientific Model Development,* 6**,** 643-685.

Piccolroaz, S., Toffolon, M. & Majone, B. 2013. A simple lumped model to convert air temperature into surface water temperature in lakes. *Hydrology and Earth System Sciences,* 17**,** 3323-3338.

Prairie, Y. T., Bird, D. F. & Cole, J. J. 2002. The summer metabolic balance in the epilimnion of southeastern Quebec lakes. *Limnology and Oceanography,* 47**,** 316-321.

Quay, P. D., Emerson, S. R., Quay, B. M. & Devol, A. H. 1986. THE CARBON-CYCLE FOR LAKE WASHINGTON - A STABLE ISOTOPE STUDY. *Limnology and Oceanography,* 31**,** 596-611.

Roiha, T., Tiirola, M., Cazzanelli, M. & Rautio, M. 2012. Carbon quantity defines productivity while its quality defines community composition of bacterioplankton in subarctic ponds. *Aquatic Sciences,* 74**,** 513-525.

Romankevich, E. A. & Vetrov, A. A. 2013. Masses of carbon in the Earth's hydrosphere. *Geochemistry International,* 51**,** 431-455.

Rouillard, A., Rosen, P., Douglas, M. S. V., Pienitz, R. & Smol, J. P. 2011. A model for inferring dissolved organic carbon (DOC) in lakewater from visible-near-infrared spectroscopy (VNIRS) measures in lake sediment. *Journal of Paleolimnology,* 46**,** 187-202.

Shao, P., Zeng, X. B., Sakaguchi, K., Monson, R. K. & Zeng, X. D. 2013. Terrestrial Carbon Cycle: Climate Relations in Eight CMIP5 Earth System Models. *Journal of Climate,* 26**,** 8744-8764.

Shaver, G., Laundre, J. & Cherry, J. 2011. Soil temperatures, lake temperature, lake depth, and evaporation pan depth and pan water temperature data from Toolik Field Station, Toolik Lake, Alaska for 2009.

Shaver, G. R. 2000. Soil temperatures, lake temperature, lake depth, and evaporation pan depth and pan water temperature data from Toolik Field Station, Toolik Lake, Alaska for 1999.

Singarayer, J. S. & Valdes, P. J. 2010. High-latitude climate sensitivity to ice-sheet forcing over the last 120 kyr. *Quaternary Science Reviews,* 29**,** 43-55.

Sitch, S., Smith, B., Prentice, I. C., Arneth, A., Bondeau, A., Cramer, W., Kaplan, J., Levis, S., Lucht, W. & Sykes, M. T. 2003. Evaluation of ecosystem dynamics, plant geography and terrestrial carbon cycling in the LPJ dynamic global vegetation model. *Global Change Biology,* 9**,** 161-185.

Smith, B. 2001. LPJ-GUESS - an ecosystem modelling framework. Available: http://www.nateko.lu.se/lpj-guess/education/html/guess.pdf [Accessed 27/8/2013].

Smith, B., Prentice, I. C. & Sykes, M. T. 2001. Representation of vegetation dynamics in the modelling of terrestrial ecosystems: comparing two contrasting approaches within European climate space. *Global Ecology and Biogeography,* 10**,** 621-637.

Snucins, E. & Gunn, J. 2000. Interannual variation in the thermal structure of clear and colored lakes. *Limnology and Oceanography,* 45**,** 1639-1646.

Sobek, S., Tranvik, L. J., Prairie, Y. T., Kortelainen, P. & Cole, J. J. 2007. Patterns and regulation of dissolved organic carbon: An

analysis of 7,500 widely distributed lakes. *Limnology and Oceanography,* 52**,** 1208-1219.
Sommer, U., Adrian, R., Domis, L. D. S., Elser, J. J., Gaedke, U., Ibelings, B., Jeppesen, E., Lurling, M., Molinero, J. C., Mooij, W. M., Van Donk, E. & Winder, M. 2012. Beyond the Plankton Ecology Group (PEG) Model: Mechanisms Driving Plankton Succession. *Annual Review of Ecology, Evolution, and Systematics, Vol 43,* 43**,** 429-448.
St Louis, V. L., Kelly, C. A., Duchemin, E., Rudd, J. W. M. & Rosenberg, D. M. 2000. Reservoir surfaces as sources of greenhouse gases to the atmosphere: A global estimate. *Bioscience,* 50**,** 766-775.
Starfield, A. M. & Chapin, F. S. 1996. Model of transient changes in arctic and boreal vegetation in response to climate and land use change. *Ecological Applications,* 6**,** 842-864.
Steinberg, C. E. W., Kamara, S., Prokhotskaya, V. Y., Manusadžianas, L., Karasyova, T. A., Timofeyev, M. A., Zhang, J., Paul, A., Meinelt, T., Farjalla, V. F., Matsuo, A. Y. O., Burnison, B. K. & Menzel, R. 2006. Dissolved humic substances – ecological driving forces from the individual to the ecosystem level? *Freshwater Biology,* 51**,** 1189-1210.
Tang, J., Pilesjö, P., Miller, P. A., Persson, A., Yang, Z., Hanna, E. & Callaghan, T. V. 2013. Incorporating topographic indices into dynamic ecosystem modelling using LPJ-GUESS. *Ecohydrology*.
Teodoru, C. R., Del Giorgio, P. A., Prairie, Y. T. & St-Pierre, A. 2013. Depositional fluxes and sources of particulate carbon and nitrogen in natural lakes and a young boreal reservoir in Northern Québec. *Biogeochemistry,* 113**,** 323-339.
Thorsteinsson, T. & Pundsack, J. 2010. Arctic-HYDRA Consortium (2010). Arctic-HYDRA: The Arctic Hydrological Cycle Monitoring, Modelling and Assessment Programme.
Tranvik, L. J., Downing, J. A., Cotner, J. B., Loiselle, S. A., Striegl, R. G., Ballatore, T. J., Dillon, P., Finlay, K., Fortino, K., Knoll, L. B., Kortelainen, P. L., Kutser, T., Larsen, S., Laurion, I., Leech, D. M., Mccallister, S. L., Mcknight, D. M., Melack, J. M., Overholt, E., Porter, J. A., Prairie, Y., Renwick, W. H., Roland, F., Sherman, B. S., Schindler, D. W., Sobek, S., Tremblay, A., Vanni, M. J., Verschoor, A. M., Von Wachenfeldt, E. & Weyhenmeyer, G. A. 2009. Lakes and reservoirs as regulators of carbon cycling and climate. *Limnology and Oceanography,* 54**,** 2298-2314.
Van Hardenbroek, M. 2014.
Vavrus, S., Waliser, D., Schweiger, A. & Francis, J. 2009. Simulations of 20th and 21st century Arctic cloud amount in the global

climate models assessed in the IPCC AR4. *Climate dynamics,* 33**,** 1099-1115.

Wania, R., Ross, I. & Prentice, I. C. 2009. Integrating peatlands and permafrost into a dynamic global vegetation model: 2. Evaluation and sensitivity of vegetation and carbon cycle processes. *Global Biogeochemical Cycles,* 23.

Wania, R., Ross, I. & Prentice, I. C. 2010. Implementation and evaluation of a new methane model within a dynamic global vegetation model: LPJ-WHyMe v1.3.1. *Geoscientific Model Development,* 3**,** 565-584.

Wetzel, R. G. 2001. *Limnology: Lake and River Ecosystems*, Elsevier Science.

Weyhenmeyer, G. A., Kortelainen, P., Sobek, S., Muller, R. & Rantakari, M. 2012. Carbon Dioxide in Boreal Surface Waters: A Comparison of Lakes and Streams. *Ecosystems,* 15**,** 1295-1307.

White, A., Cannell, M. G. R. & Friend, A. D. 2000. The high-latitude terrestrial carbon sink: a model analysis. *Global Change Biology,* 6**,** 227-245.

Willey, J. D., Kieber, R. J., Eyman, M. S. & Avery, G. B. 2000. Rainwater dissolved organic carbon: Concentrations and global flux. *Global Biogeochemical Cycles,* 14**,** 139-148.

Wolf, A., Callaghan, T. V. & Larson, K. 2008. Future changes in vegetation and ecosystem function of the Barents Region. *Climatic change,* 87**,** 51-73.

Wolter, P. T., Johnston, C. A. & Niemi, G. J. 2005. Mapping submergent aquatic vegetation in the US Great Lakes using Quickbird satellite data. *International Journal of Remote Sensing,* 26**,** 5255-5274.

Woodward, F. 1987. *Climate and Plant Distribution,* Cambridge, Cambridge University Press.

Wu, H., Peng, C., Lucotte, M., Soumis, N., Gélinas, Y., Duchemin, É., Plouhinec, J. B., Ouellet, A. & Guo, Z. 2013. A coupled two-dimensional hydrodynamic and terrestrial input model to simulate CO2 diffusive emissions from lake systems. *Geosci. Model Dev. Discuss.,* 6**,** 3509-3556.

Zhang, C., Jamieson, R. C., Meng, F.-R., Gordon, R. J. & Bourque, C. P. A. 2013a. Simulation of monthly dissolved organic carbon concentrations in small forested watersheds. *Ecological Modelling,* 250**,** 205-213.

Zhang, W., Miller, P. A., Smith, B., Wania, R., Koenigk, T. & Doscher, R. 2013b. Tundra shrubification and tree-line advance amplify arctic climate warming: results from an individual-based dynamic vegetation model. *Environmental Research Letters,* 8.